

Electronic Supplementary Information

Tetravalent Cerium Pseudohalide Complexes Supported by the Kläui Tripodal Ligand $[\text{Co}(\eta^5\text{-C}_5\text{H}_5)\{\text{P}(\text{O})(\text{OEt})_2\}_3]^-$

Ka-Chun Au-Yeung, Yat-Ming So, Herman H.-Y. Sung, Ian D. Williams and Wa-Hung Leung**

Contents

1. Crystallographic data and experimental details for complexes **2**, **3**, **6** and **9**
2. Preliminary X-ray structure of **5**
3. Preliminary X-ray structure of **8**
4. XPS spectrum of **9**
5. NMR spectra of **2-4** and **6-9**
6. IR spectra of **2-9**
7. Electronic absorption spectra of **1-4**
8. Cyclic voltammograms of complexes **2** and **3**.

Table S1. Crystallographic data and experimental details for complexes **2**, **3**, **6** and **9**

	2·3CH₂Cl₂	3	6·½C₄H₁₀O	9·C₆H₁₄
Formula	C ₃₉ H ₇₆ CeCo ₂ N ₂ O ₁₈ P ₆ S ₂ Cl ₆	C ₃₄ H ₇₀ CeCo ₂ N ₆ O ₁₈ P ₆	C ₇₄ H ₁₀₅ B ₂ CeCo ₂ N ₂ O _{18.5} P ₆	C ₇₂ H ₁₄₇ Ce ₄ Co ₄ N ₁₈ O ₃₉ P ₁₂
<i>F</i> _w	1580.63	1294.76	1784.02	3044.9
Crystal system	Orthorhombic	Monoclinic	Orthorhombic	Orthorhombic
Space group	Pnma	P2 ₁ /n	Pna2 ₁ /n	Pbcn
<i>a</i> (Å)	24.4099(3)	11.57(13)	53.8313(8)	23.9797(3)
<i>b</i> (Å)	19.0973(18)	23.4809(3)	13.7543(14)	20.7737(2)
<i>c</i> (Å)	13.8324(15)	19.3336(2)	22.3077(2)	24.0697(3)
<i>α</i> , (°)	90	90	90	90
<i>β</i> , (°)	90	90.8133(12)	90	90
<i>γ</i> , (°)	90	90	90	90
<i>V</i> (Å ³)	6448.18(12)	5251.91(10)	16516.9(3)	11990.2(2)
<i>Z</i>	4	4	8	4
<i>ρ</i> _{calcd} (g cm ⁻¹)	1.628	1.638	1.435	1.687
<i>T</i> (K)	99.9(5)	100	99.9(5)	99.9(5)
<i>F</i> (000)	3212	2648	7384	6124.0
<i>μ</i> (mm ⁻¹)	14.177	13.815	8.939	2.265
No. of reflns	34924	23456	91912	67634
No. of indep reflns	5878	9243	26902	11701
<i>R</i> _{int}	0.1552	0.0605	0.0896	0.0533
GoF ^a	1.001	1.001	1.001	1.003
<i>R</i> ₁ ^b , w <i>R</i> ₂ ^c (<i>I</i> > 2σ(<i>I</i>))	0.0543, 0.1181	0.0606, 0.1476	0.0576, 0.1204	0.0466, 0.1208
<i>R</i> ₁ , w <i>R</i> ₂ (all data)	0.0816, 0.1288	0.0826, 0.1596	0.0827, 0.1304	0.0649, 0.1309

^a GoF = [Σ*w*(|*F*_o| - |*F*_c|)²/(*N*_{obs} - *N*_{param})]^{1/2}, ^b *R*₁ = Σ ||*F*_o| - |*F*_c|| / Σ |*F*_o|, ^c w*R*₂ = [Σ*w*(|*F*_o²| - |*F*_c²|)² / Σ*w*|*F*_o²|²]^{1/2}.

Figure S1. Preliminary X-ray structure of **5** showing the repeating unit $\{\text{Ce}^{\text{IV}}(\text{LOEt})_2\}\{\mu\text{-Ag}(\text{CN})_2\}(\text{AgCl}_2)$. The Ce atoms are linked together via the cyano groups of the $[\text{Ag}(\text{CN})_2]^-$ unit. Hydrogen atoms of the LOEt^- ligands are omitted for clarity. The ellipsoids are drawn at 30% probability level ($R_1 = 6.33\%$)

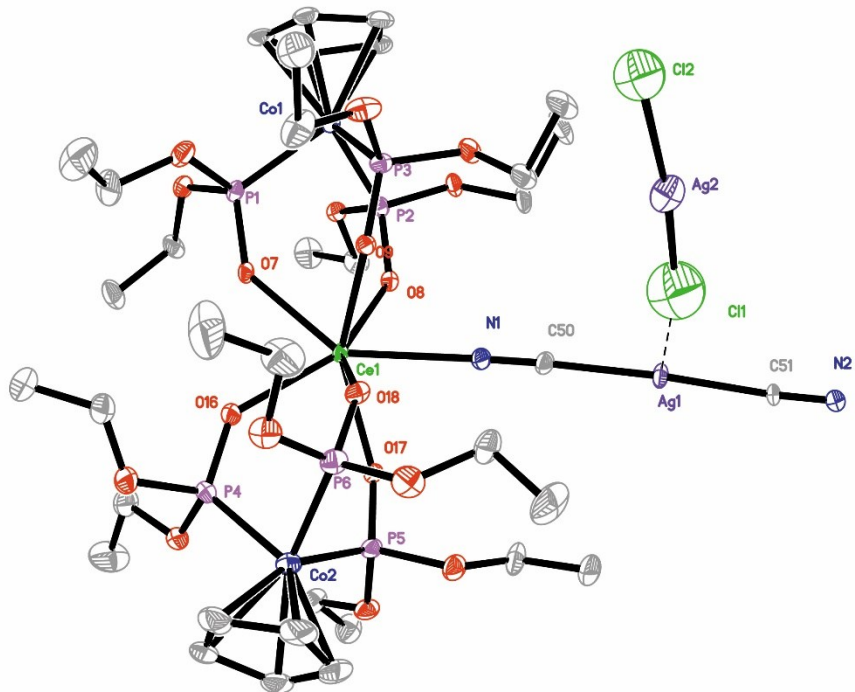


Figure S2. Preliminary X-ray structure of **8**. Hydrogen atoms of the L_{OEt}^- ligands are omitted for clarity. The ellipsoids are drawn at 30% probability level ($R_1 = 6.35\%$)

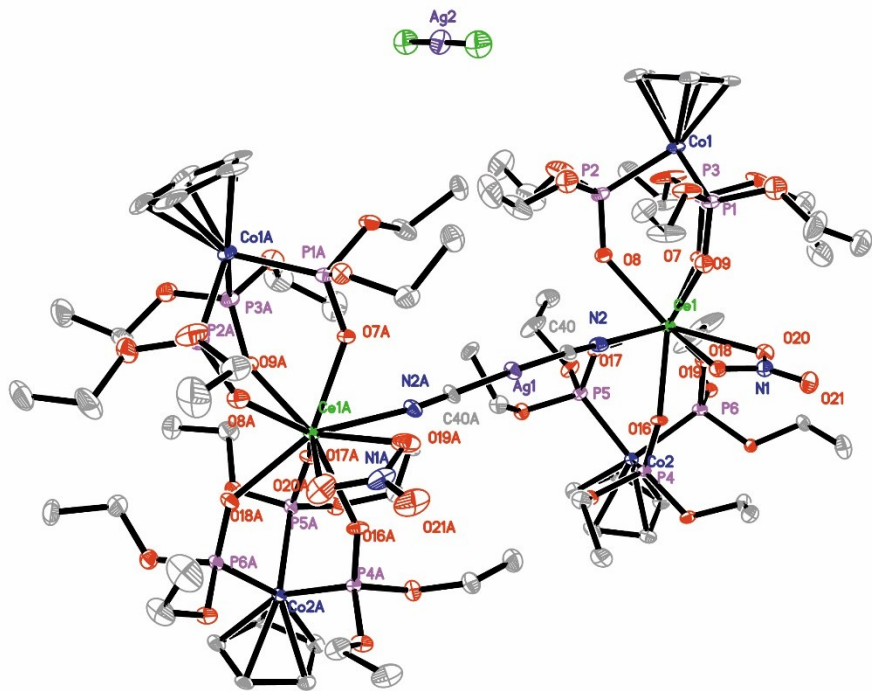


Table S2. Crystallographic data for the preliminary X-ray structures of **5** and **8**

	5	8
Formula	$\text{Ag}_4\text{C}_{78}\text{Ce}_2\text{H}_{152}\text{Cl}_{16}\text{Co}_4\text{N}_4\text{O}_{36}\text{P}_{12}$	$\text{C}_{70}\text{H}_{140}\text{Ag}_2\text{Ce}_2\text{Cl}_2\text{Co}_4\text{N}_4\text{O}_{42}\text{P}_{12}$
F_w	3608.31	2884.09
Crystal system	Monoclinic	Monoclinic
Space group	P2 ₁ /c	P2 ₁ /c
a (Å)	13.2536(3)	11.66174(11)
b (Å)	19.2946(3)	39.9468(3)
c (Å)	26.5988(7)	23.73426(18)
α , (°)	90	90
β , (°)	91.280(2)	96.7587(8)
γ , (°)	90	90
V (Å ³)	6800.2(3)	10979.76(16)
Z	2	4
ρ_{calcd} (g cm ⁻¹)	1.762	1.745
T (K)	293(2)	293(2)
$F(000)$	3600.0	5824.0
μ (mm ⁻¹)	2.214	16.477
No. of reflns	42452	48430
No. of indep reflns	15918	21809
R_{int}	0.0439	0.0435
GoF ^a	1.056	1.020
$R_1^{\text{b}}, \text{w}R_2^{\text{c}}(I > 2\sigma(I))$	0.0633, 0.1543	0.0635, 0.1601
$R_1, \text{w}R_2$ (all data)	0.0984, 0.1741	0.0850, 0.1771

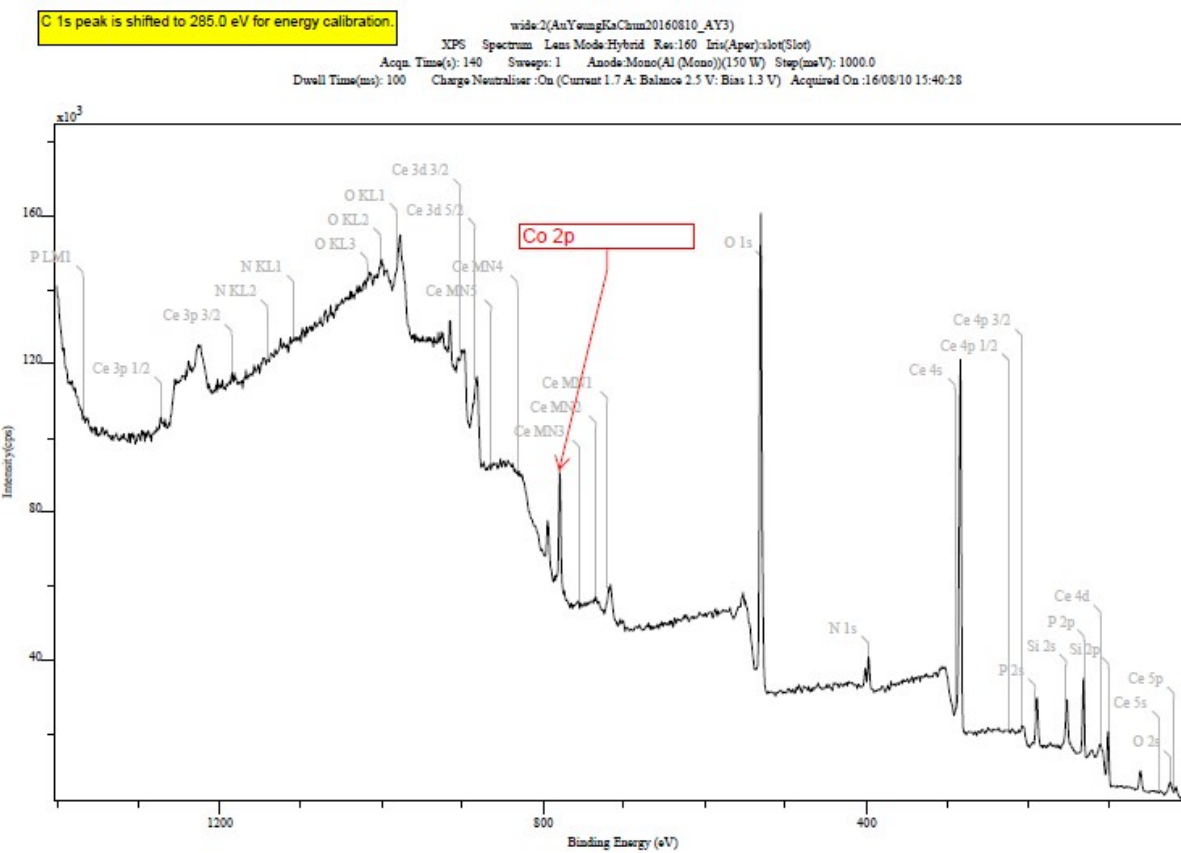


Figure S3. Full XPS spectrum of **9**

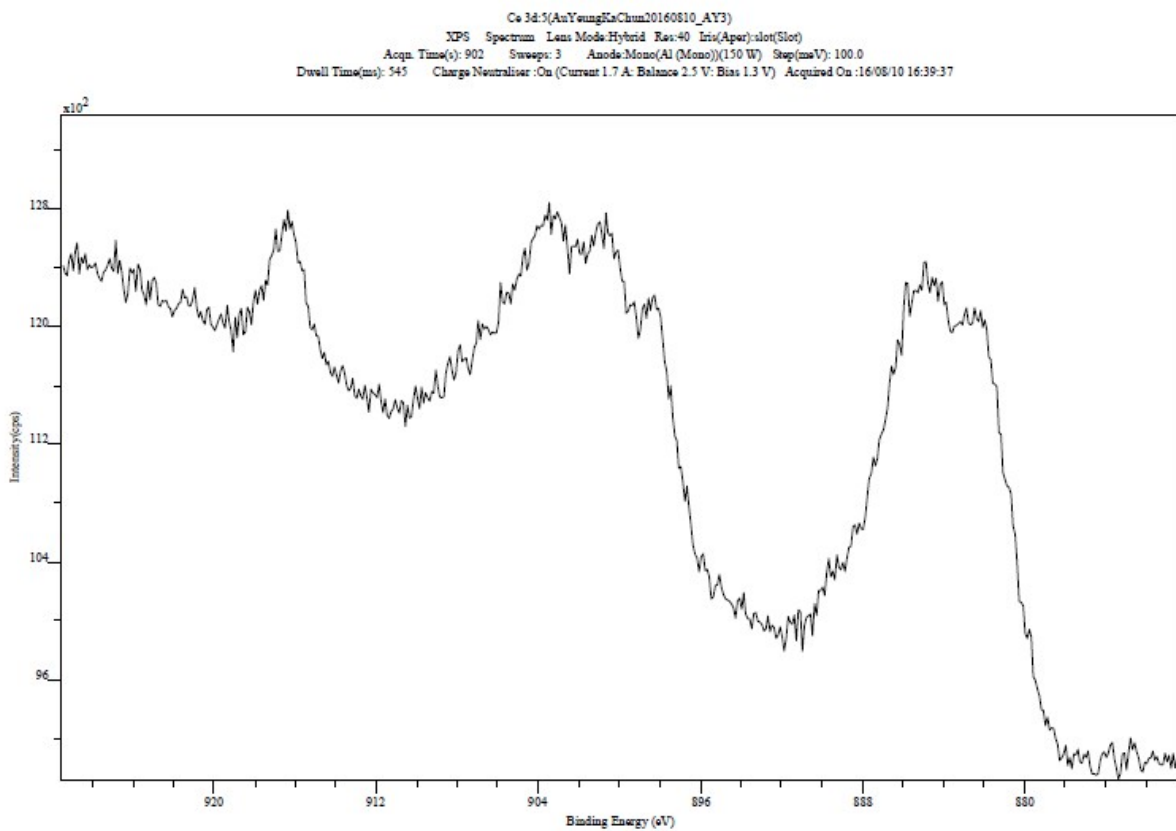


Figure S4. The Ce region of the XPS spectrum of **9**

The XPS spectrum was obtained on a Kratos Axis Ultra DLD instrument. The observed signal at ca. 916 eV is characteristic of Ce(IV) (cf. lit. 917 eV^a). No signal at ca. 880 eV that is characteristic of Ce(III) was observed, thus indicating all the Ce centers in **9** are Ce⁴⁺.

^aBeche *et al.*, *Surf. Interface Anal.* 2008, **40**, 264–267.

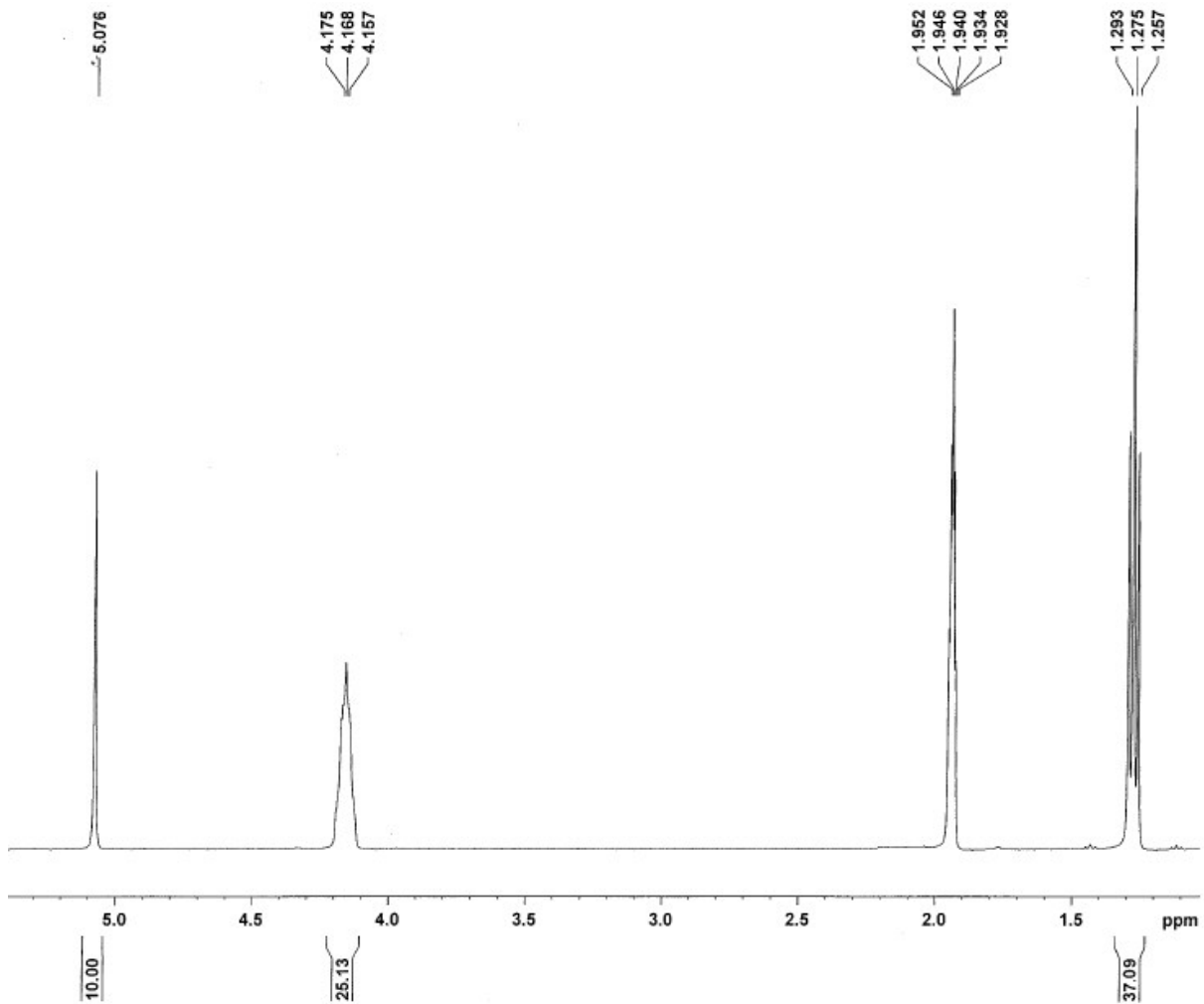


Figure S5. ${}^1\text{H}$ NMR spectrum (400 MHz, CD_3CN , 298 K) of **2**.

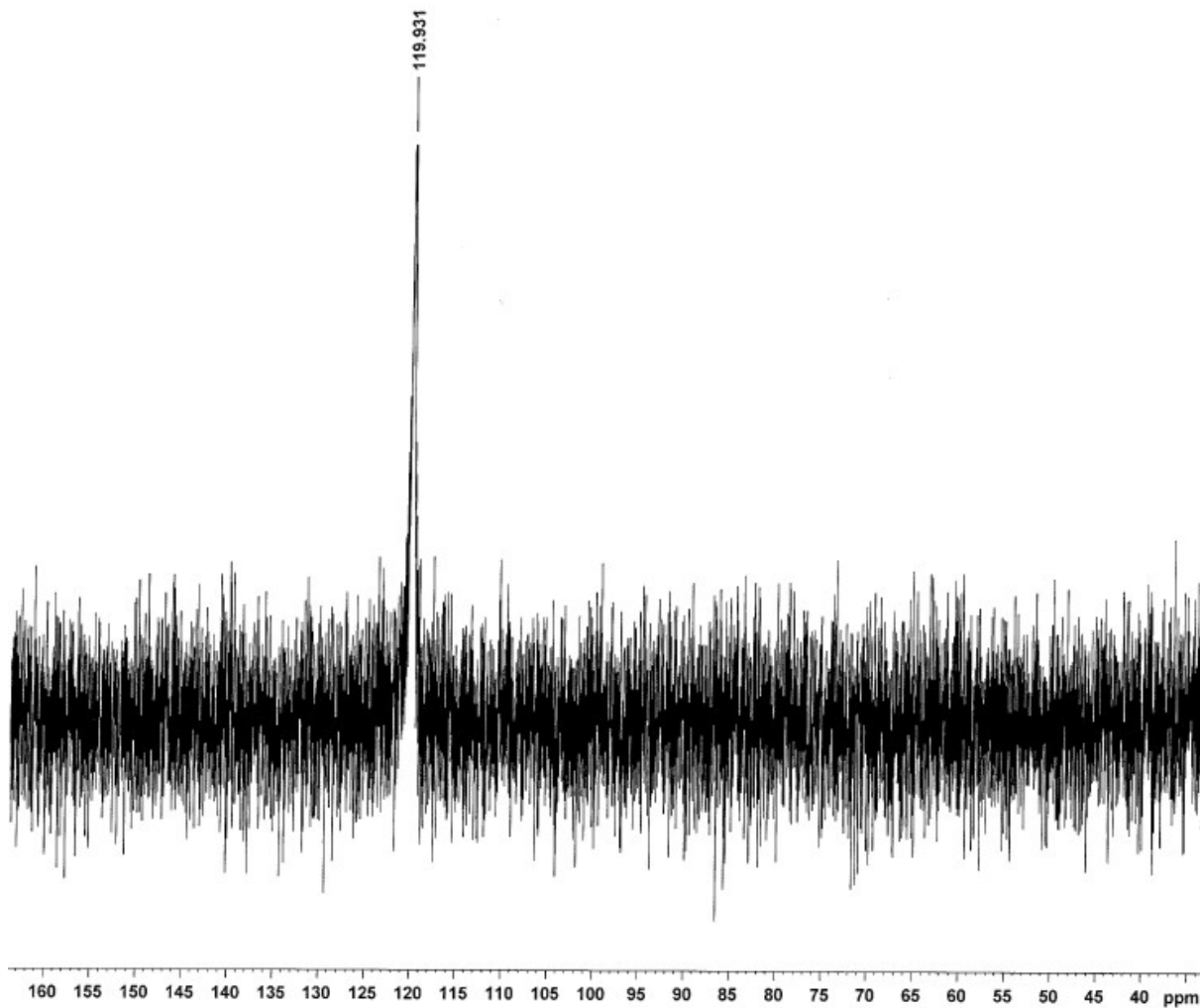


Figure S6. ^{31}P $\{^1\text{H}\}$ NMR spectrum (160 MHz, CD_3CN , 298 K) of **2**.

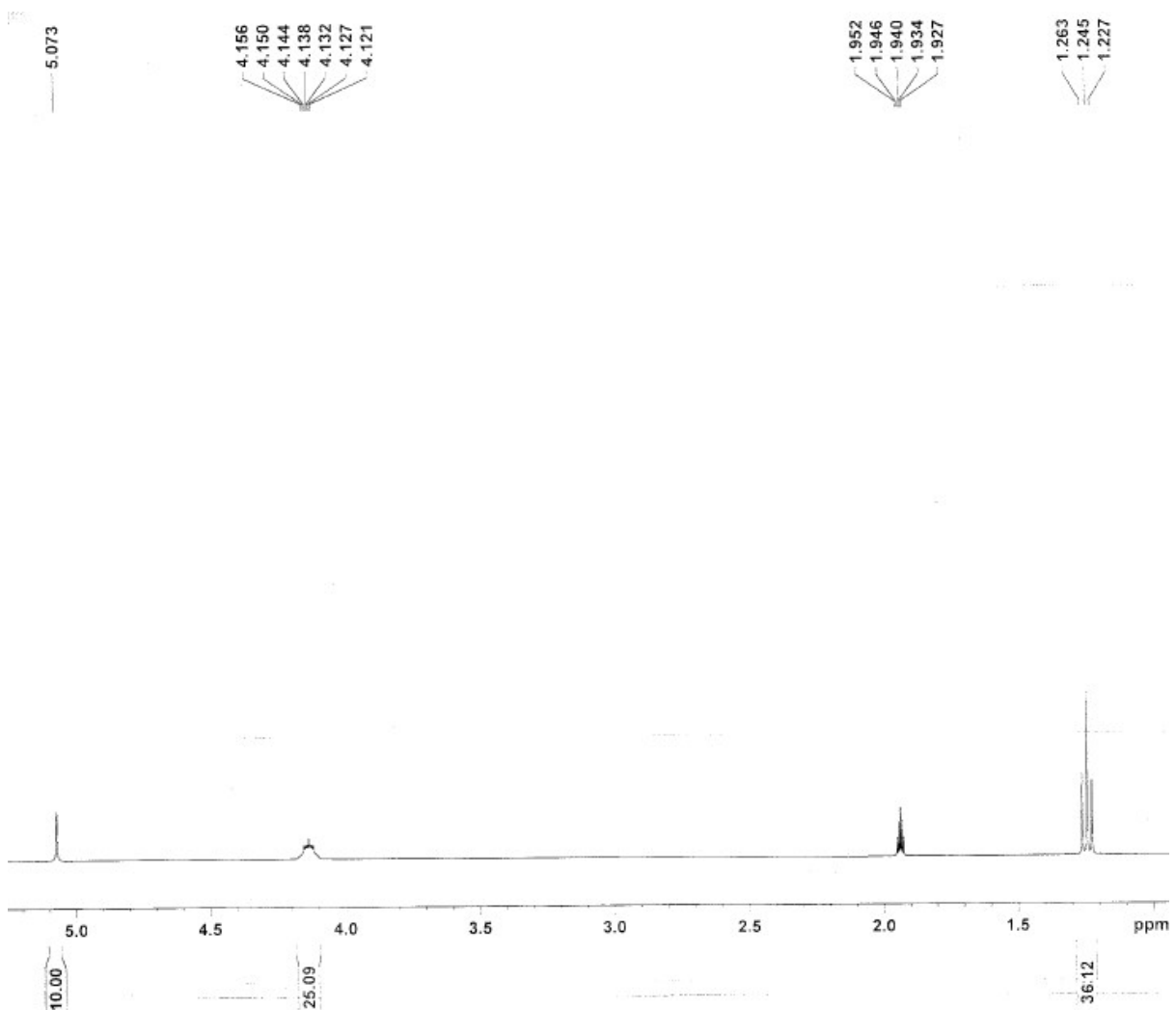


Figure S7. ${}^1\text{H}$ NMR spectrum (400 MHz, CD_3CN , 298 K) of **3**.

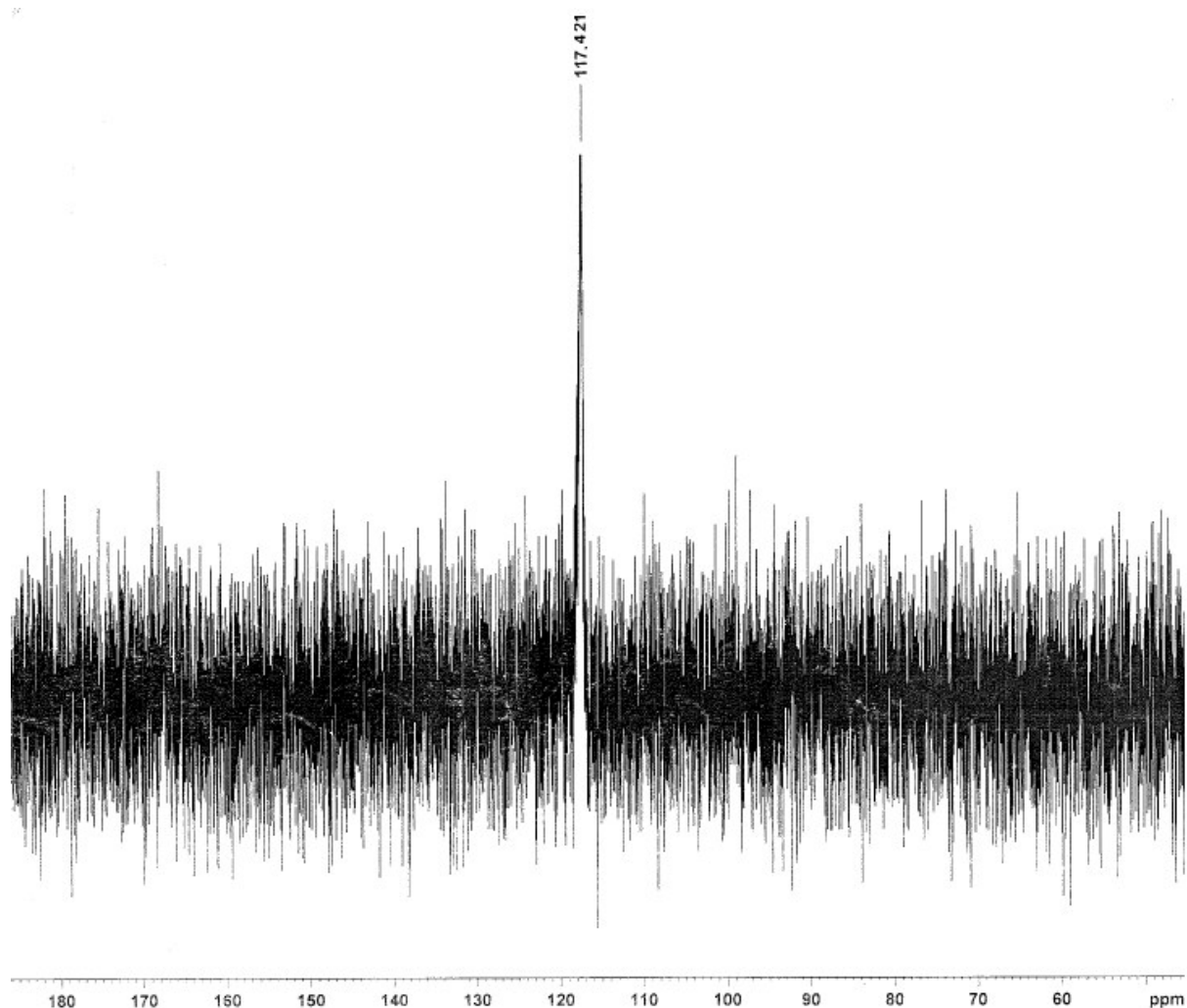


Figure S8. ^{31}P $\{^1\text{H}\}$ NMR spectrum (160 MHz, CD_3CN , 298 K) of **3**.

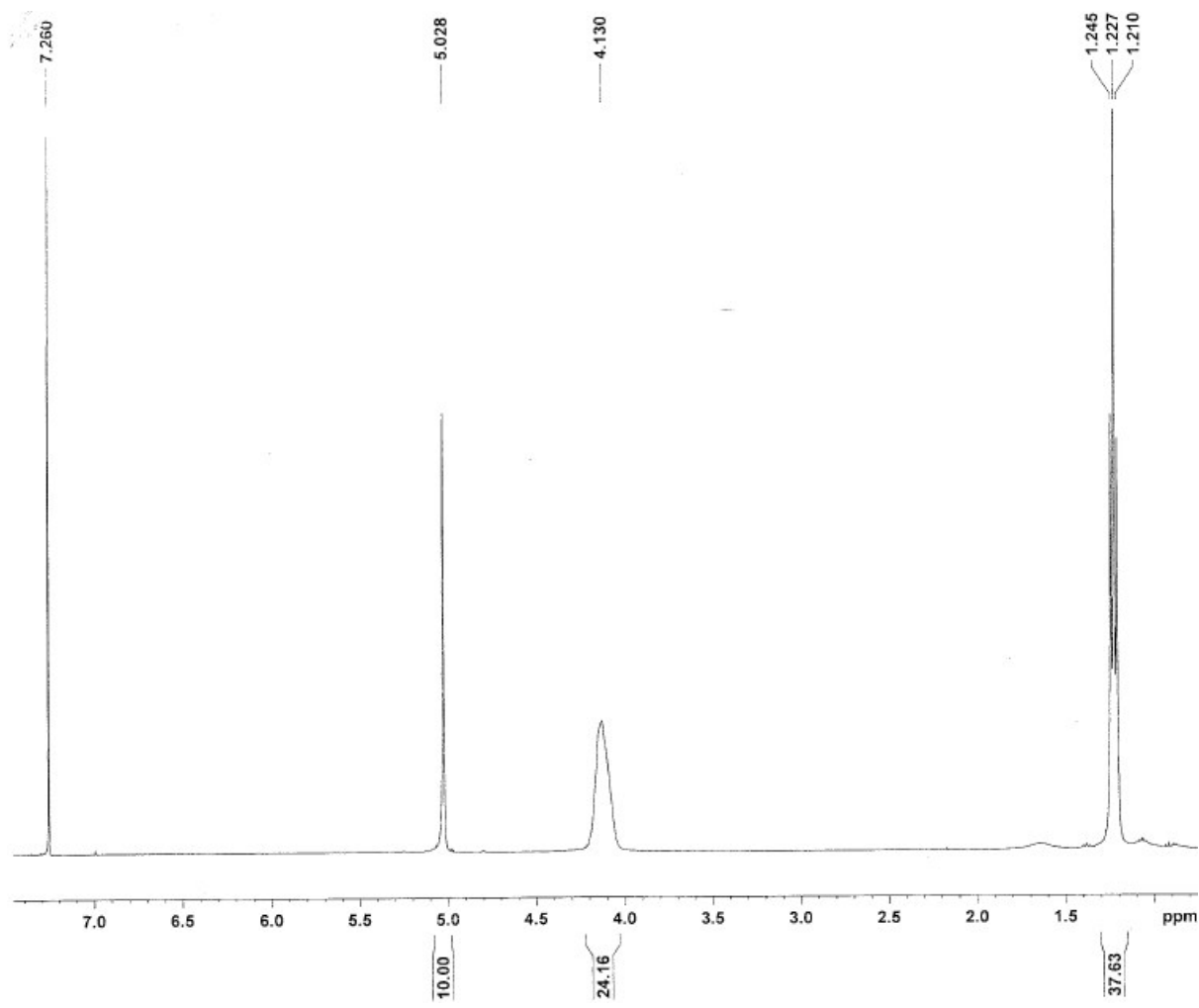


Figure S9. ^1H NMR spectrum (400 MHz, CDCl_3 , 298 K) of **4**.

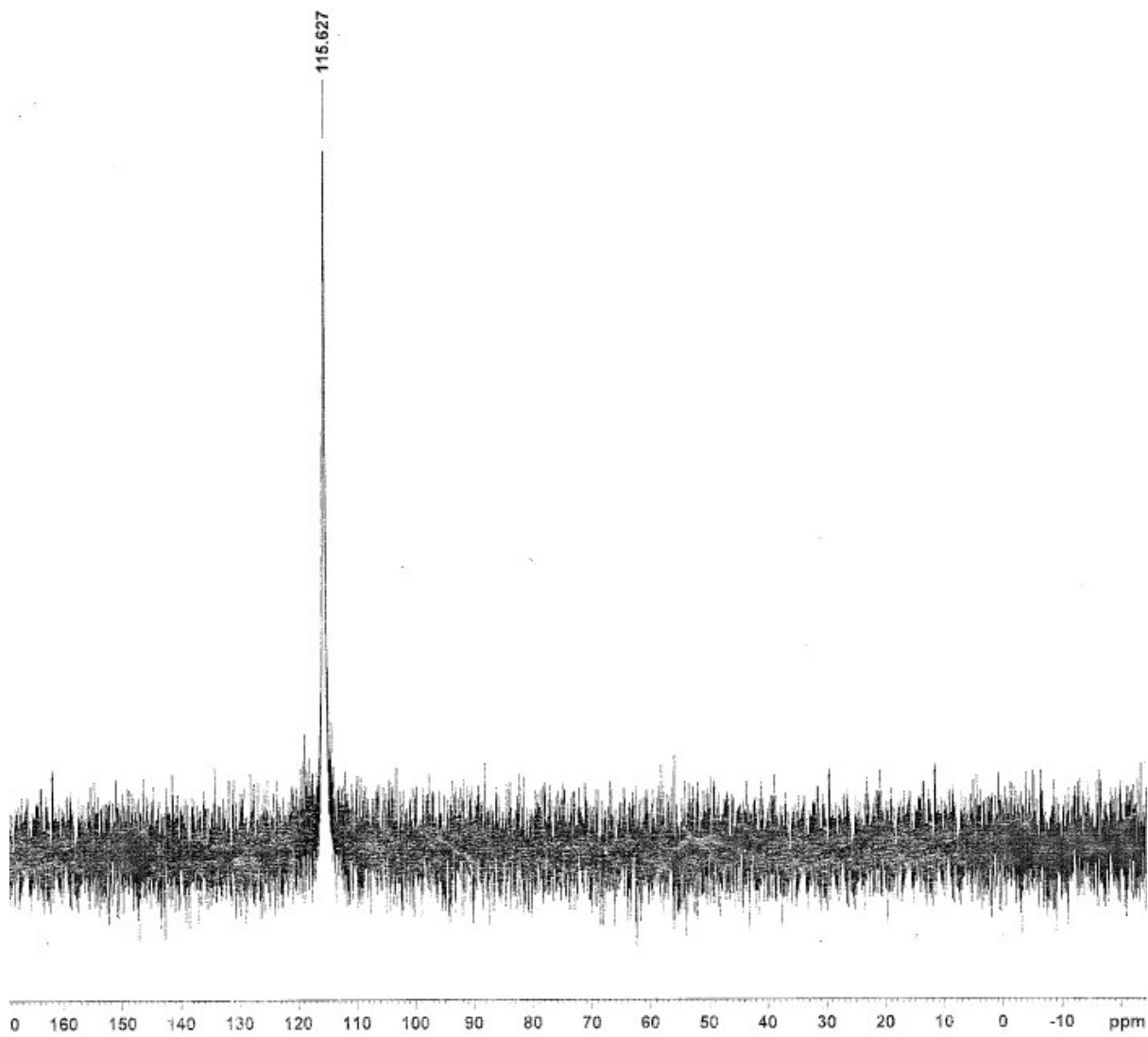


Figure S10. ^{31}P $\{\text{H}\}$ NMR spectrum (160 MHz, CDCl_3 , 298 K) of **4**.

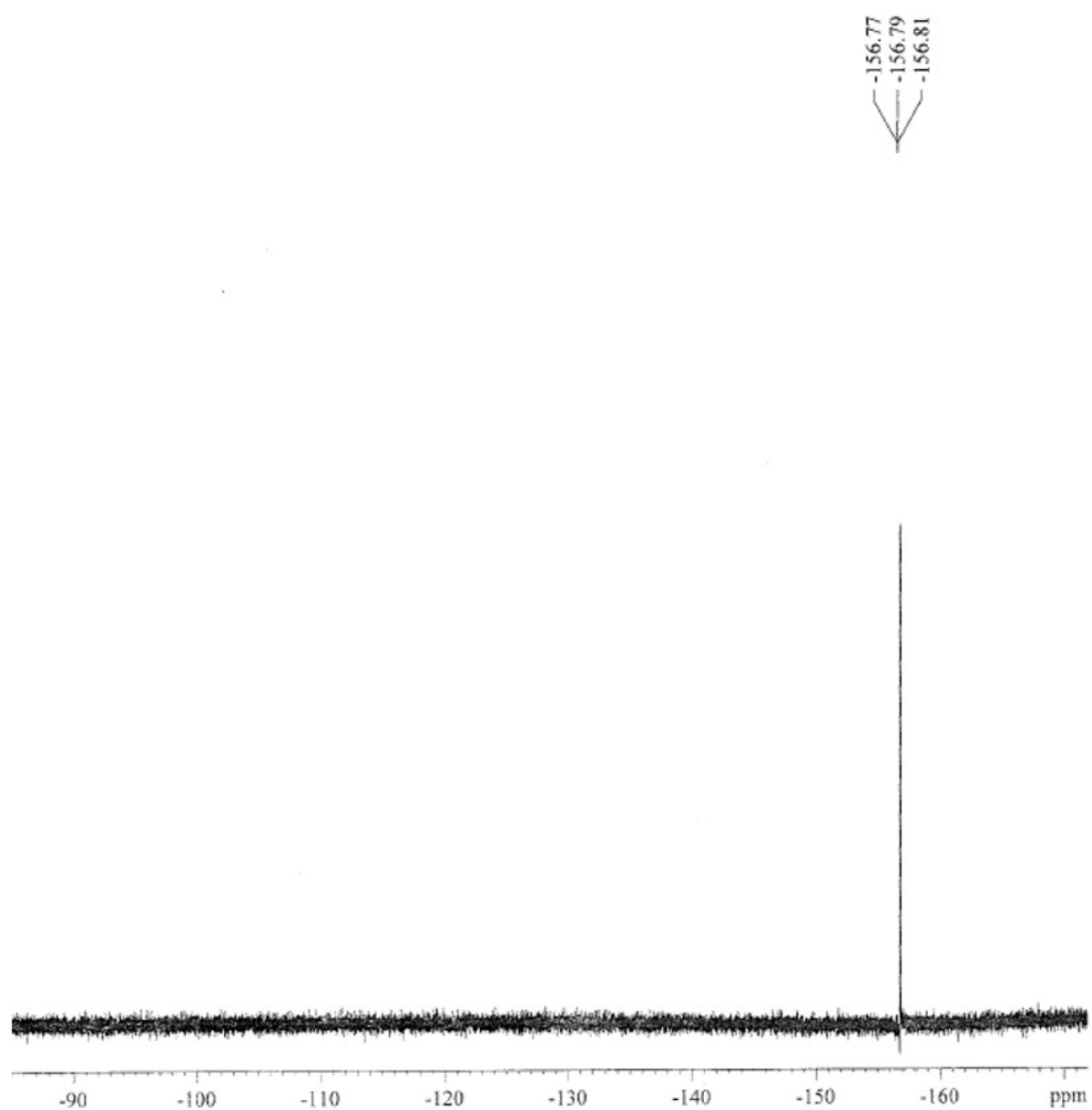


Figure S11. ${}^{19}\text{F}$ $\{{}^1\text{H}\}$ NMR (376.4 MHz, CDCl_3 , 25 °C) spectrum of **4**.

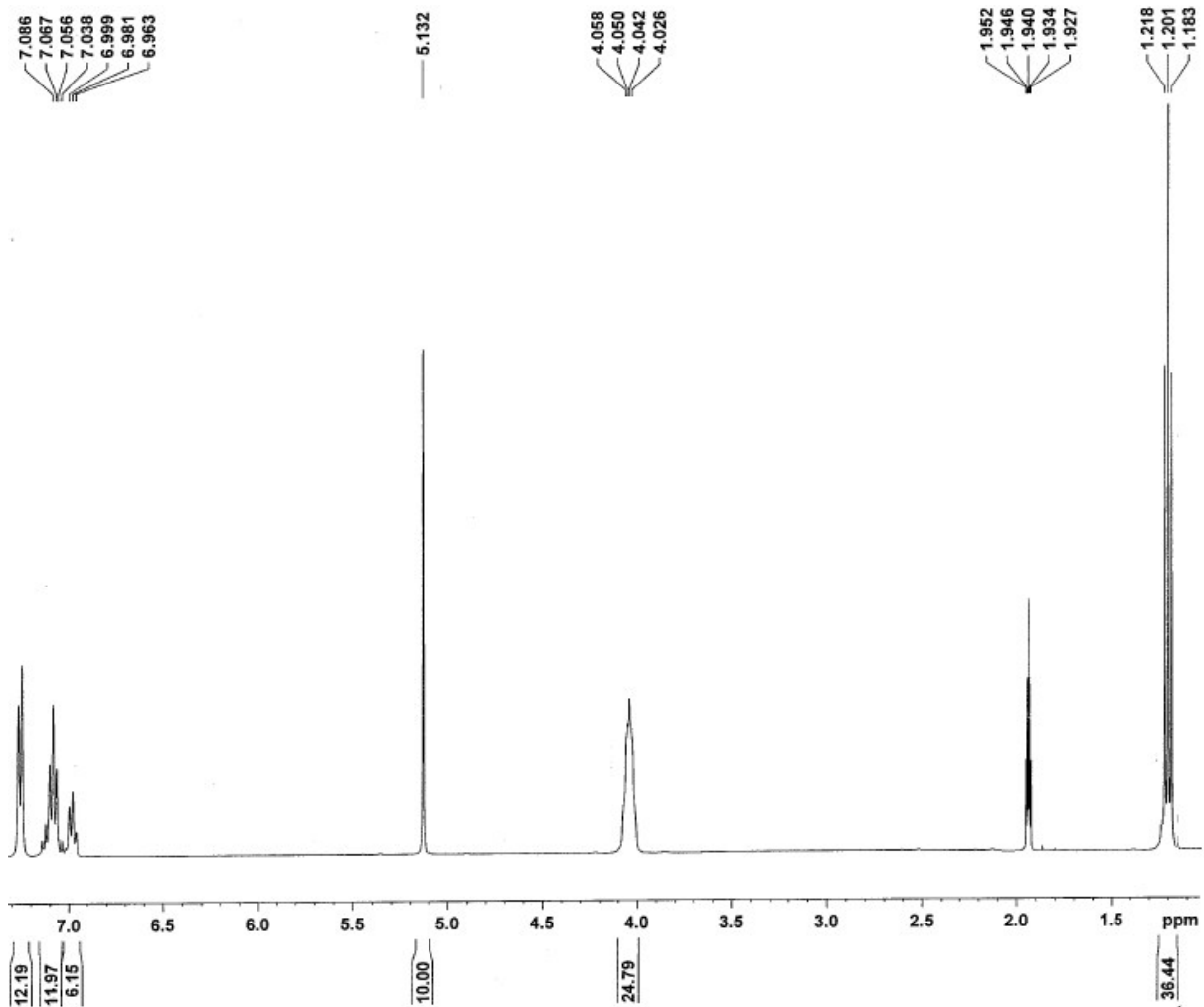


Figure S12. ^1H NMR spectrum (400 MHz, CD_3CN , 298 K) of **6**.

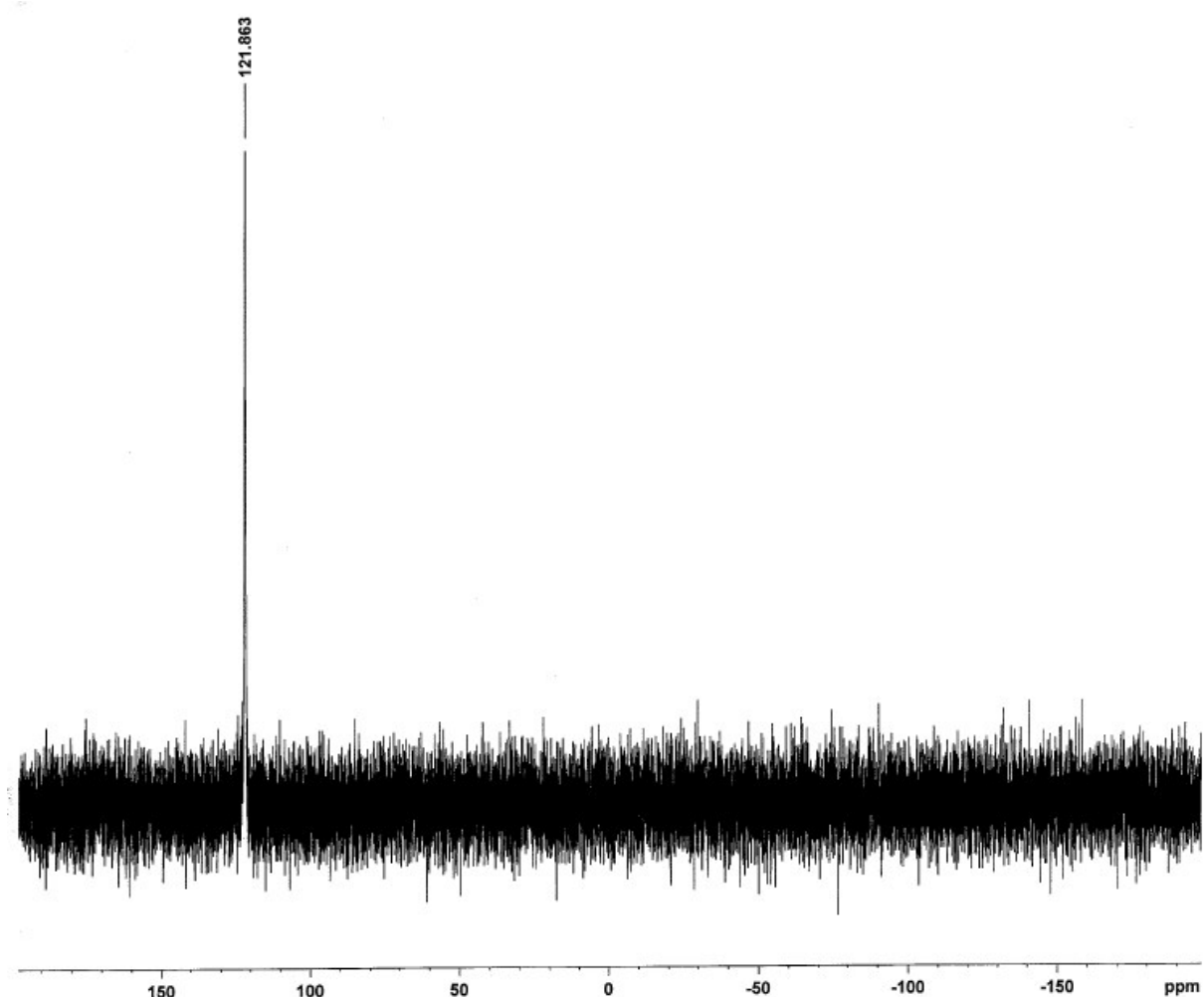


Figure S13. ^{31}P $\{^1\text{H}\}$ NMR spectrum (160 MHz, CD_3CN , 298 K) of **6**.

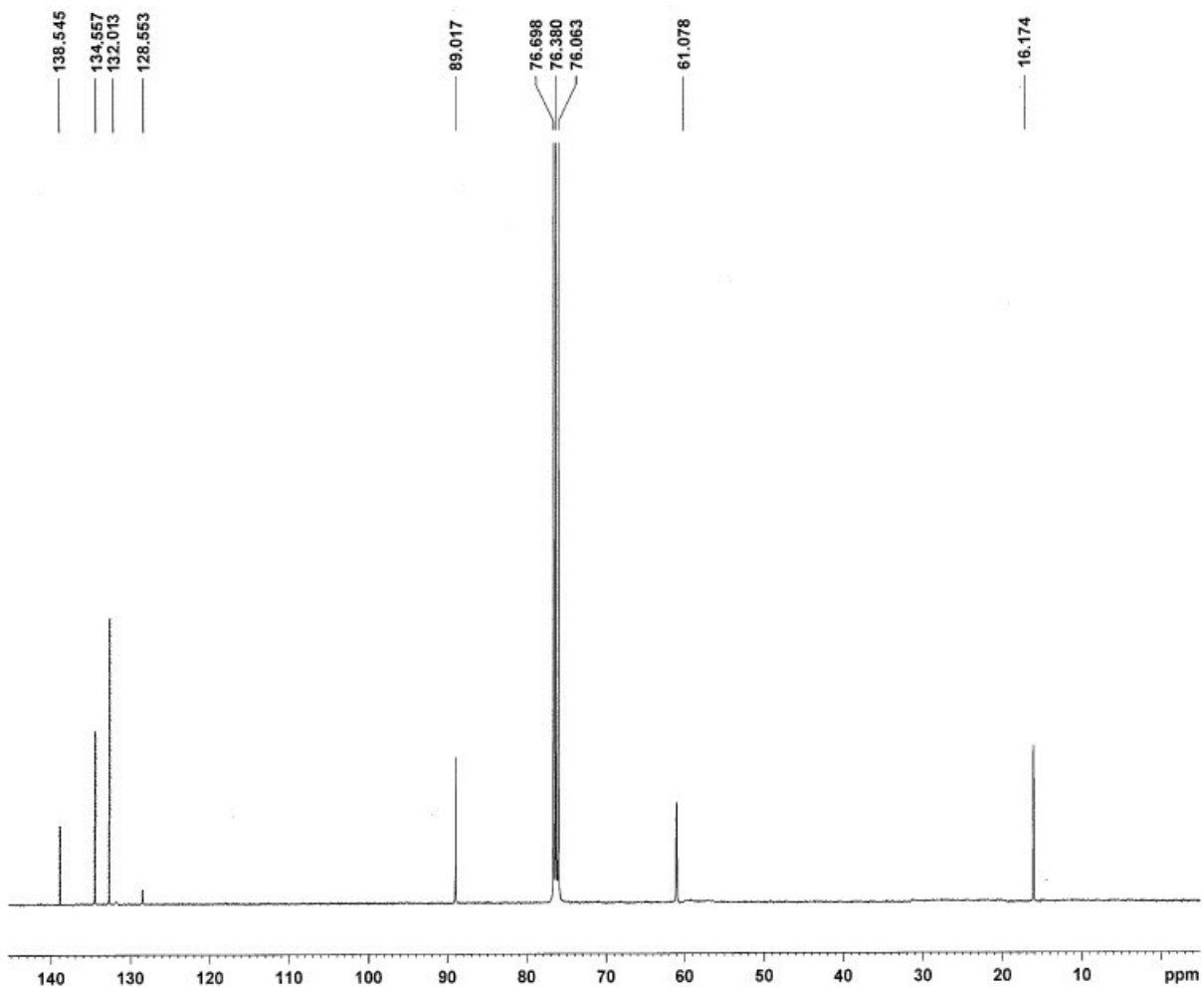


Figure S14. $^{13}\text{C}\{\text{H}\}$ NMR spectrum (100 MHz, CD_3CN , 298 K) of **6**.

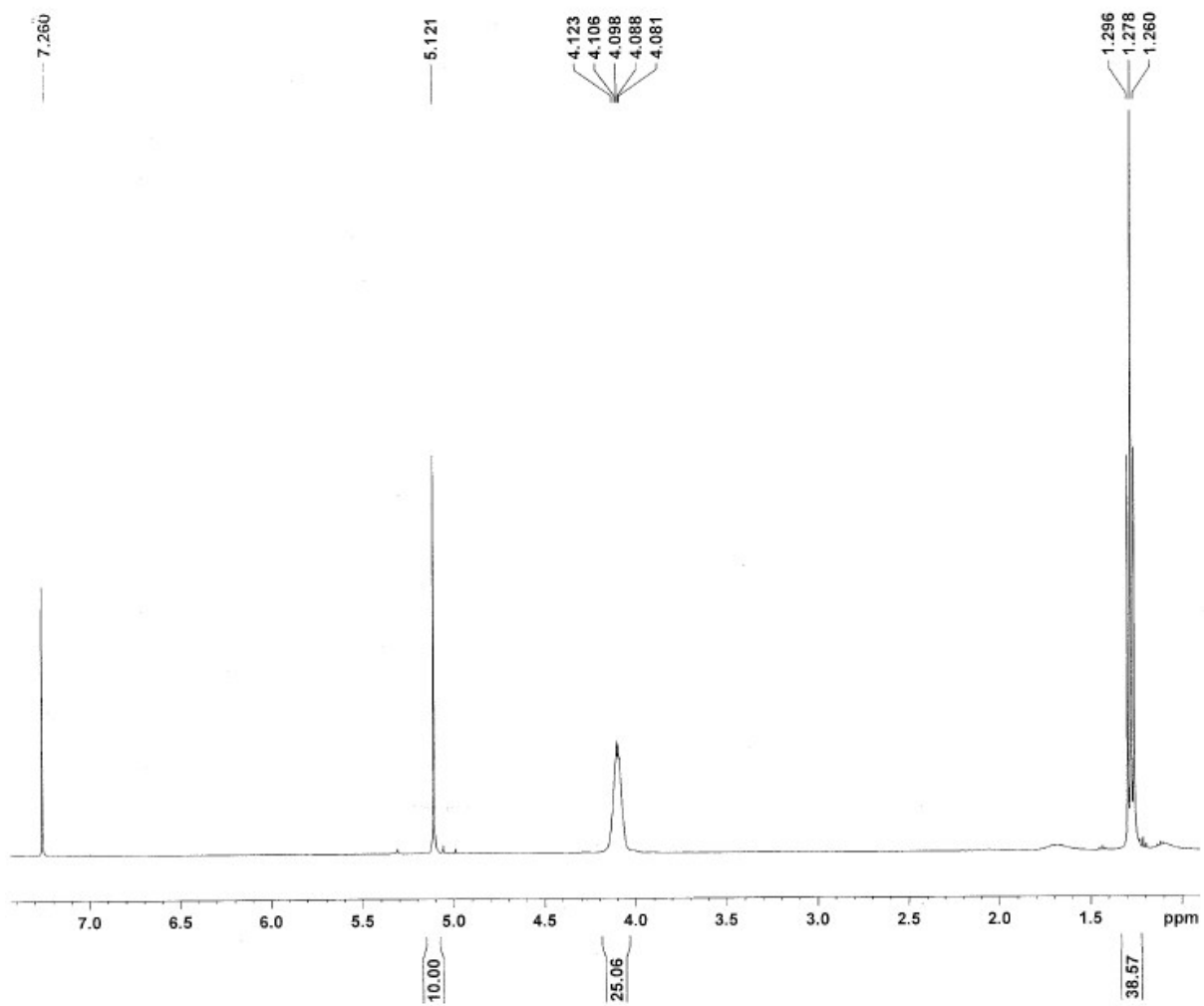


Figure S15. ${}^1\text{H}$ NMR spectrum (400 MHz, CDCl_3 , 298 K) of 7.

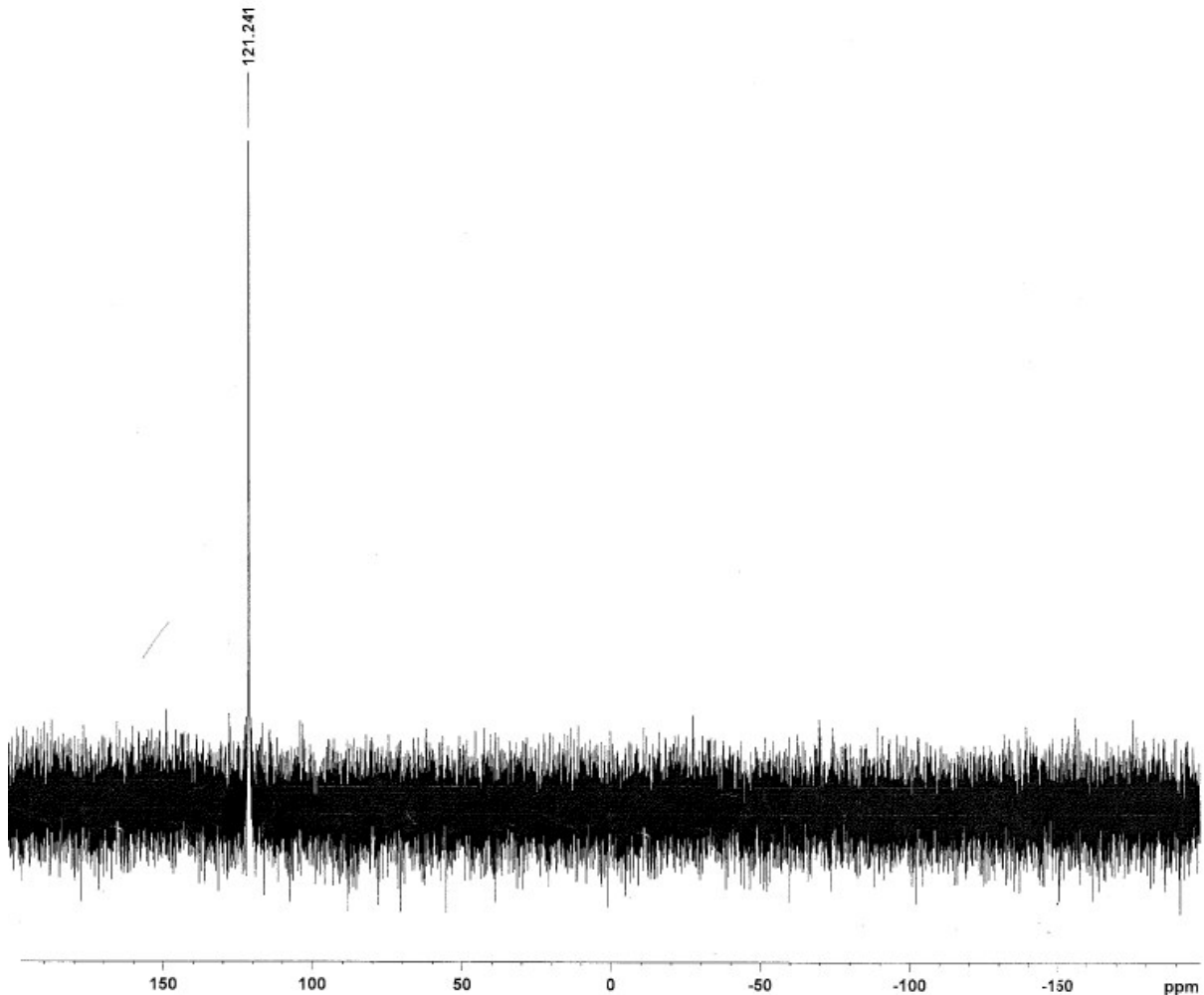


Figure S16. ^{31}P { ^1H } NMR spectrum (160 MHz, CDCl_3 , 298K) of **7**.

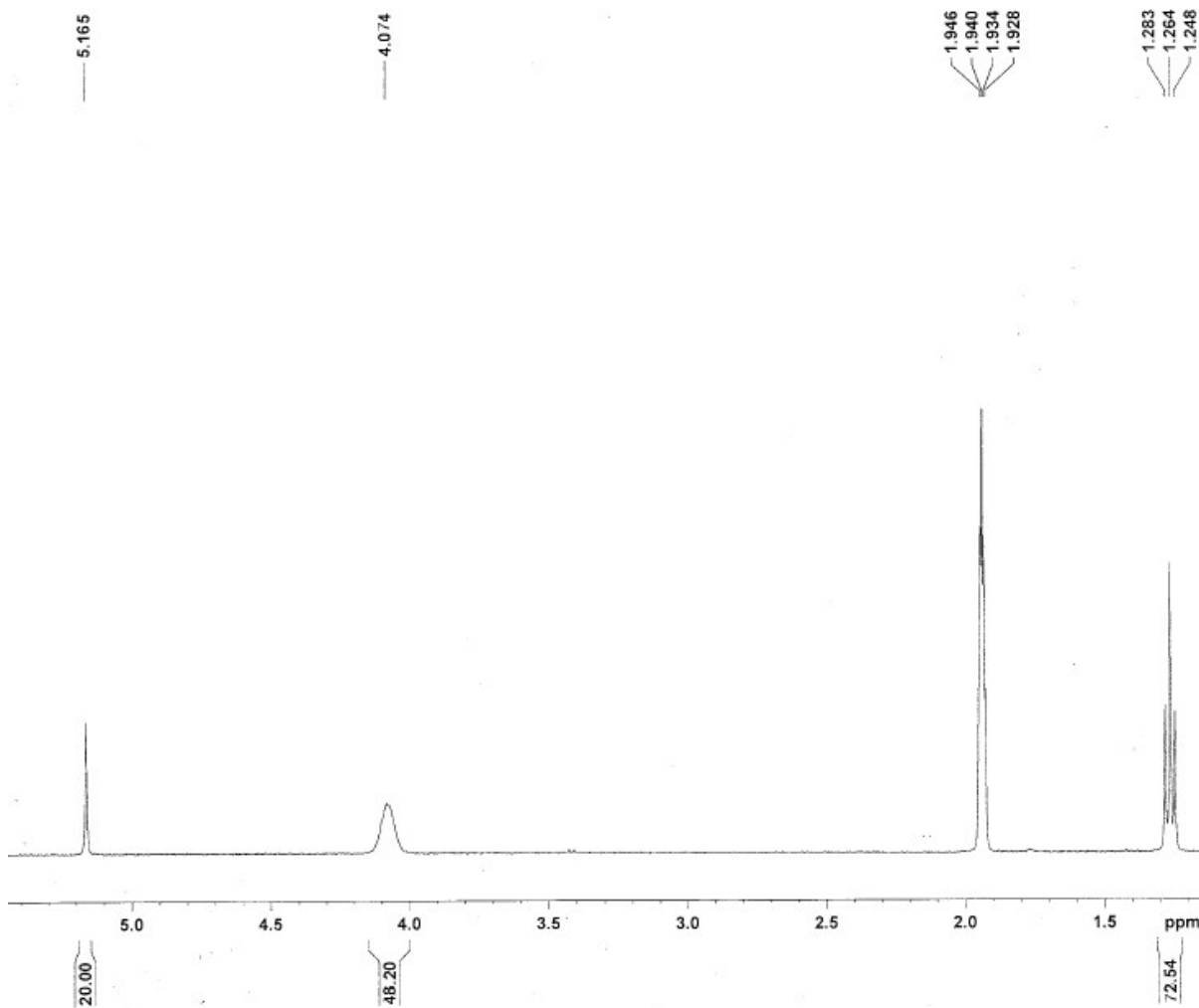


Figure S17. ^1H NMR spectrum (400 MHz, CD_3CN , 298 K) of **8**.

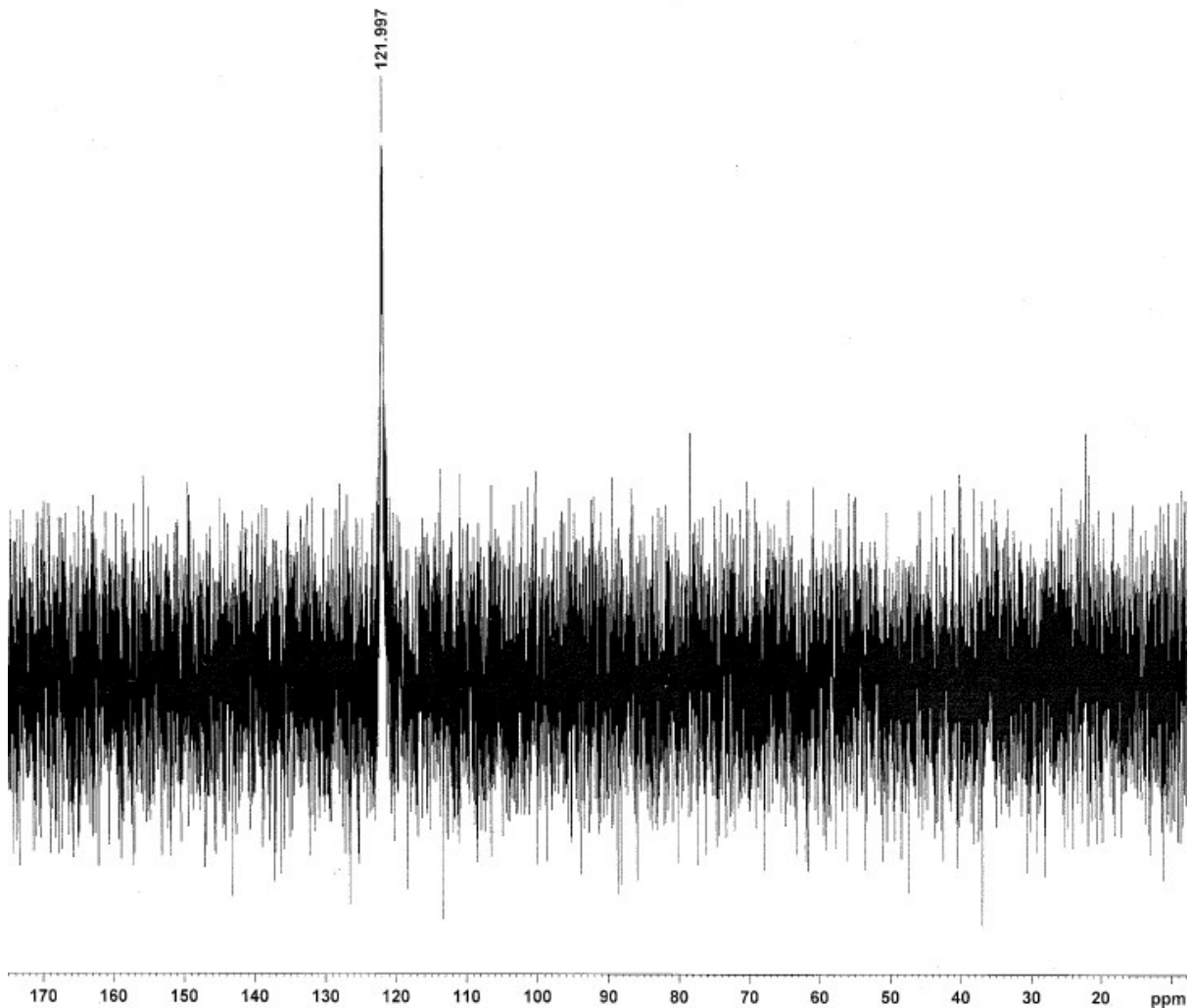


Figure S18. $^{31}\text{P} \{^1\text{H}\}$ NMR spectrum (160 MHz, CD_3CN , 298K) of **8**.

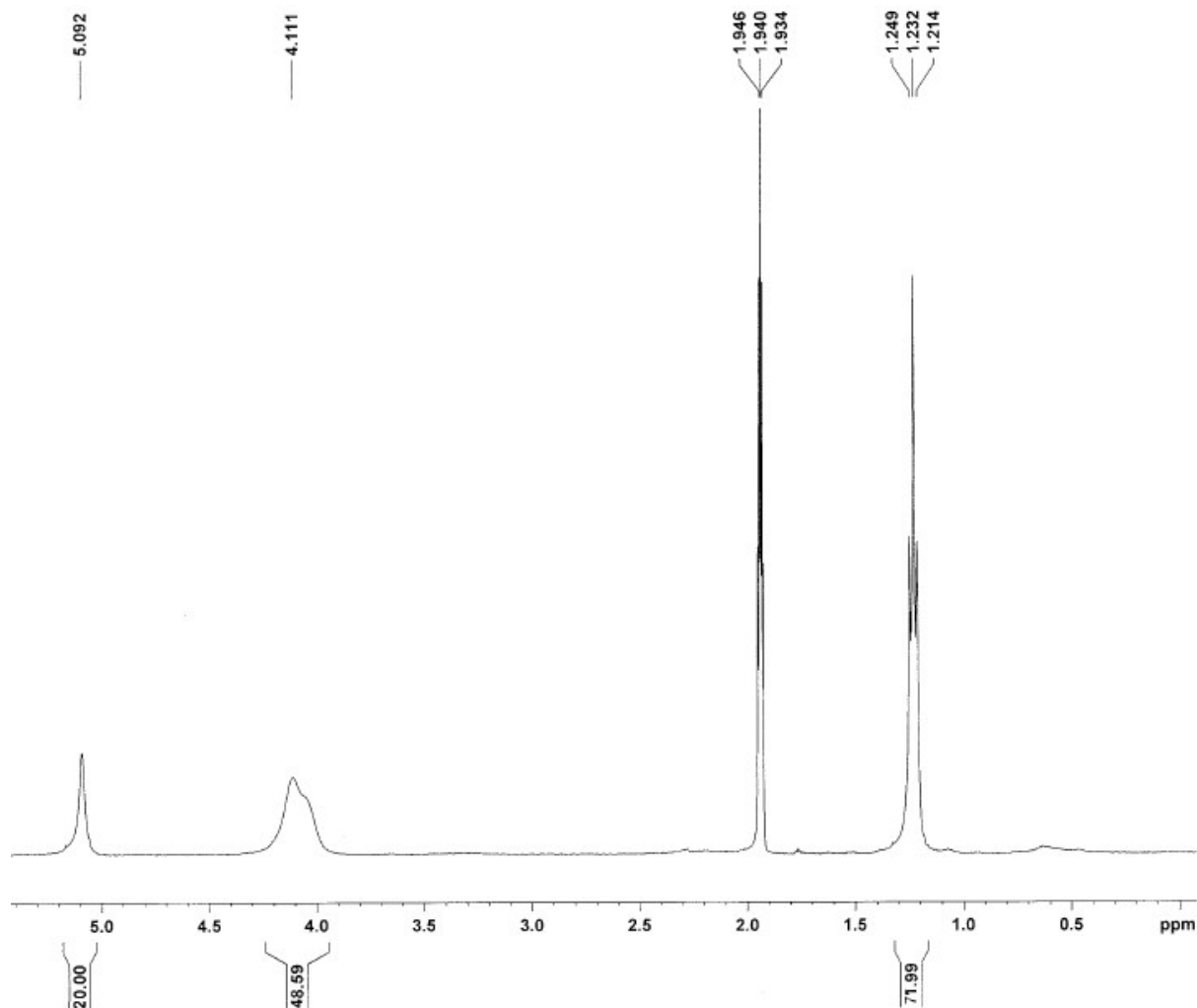


Figure S19. ${}^1\text{H}$ NMR spectrum (400 MHz, CD_3CN , 298 K) of **9**.

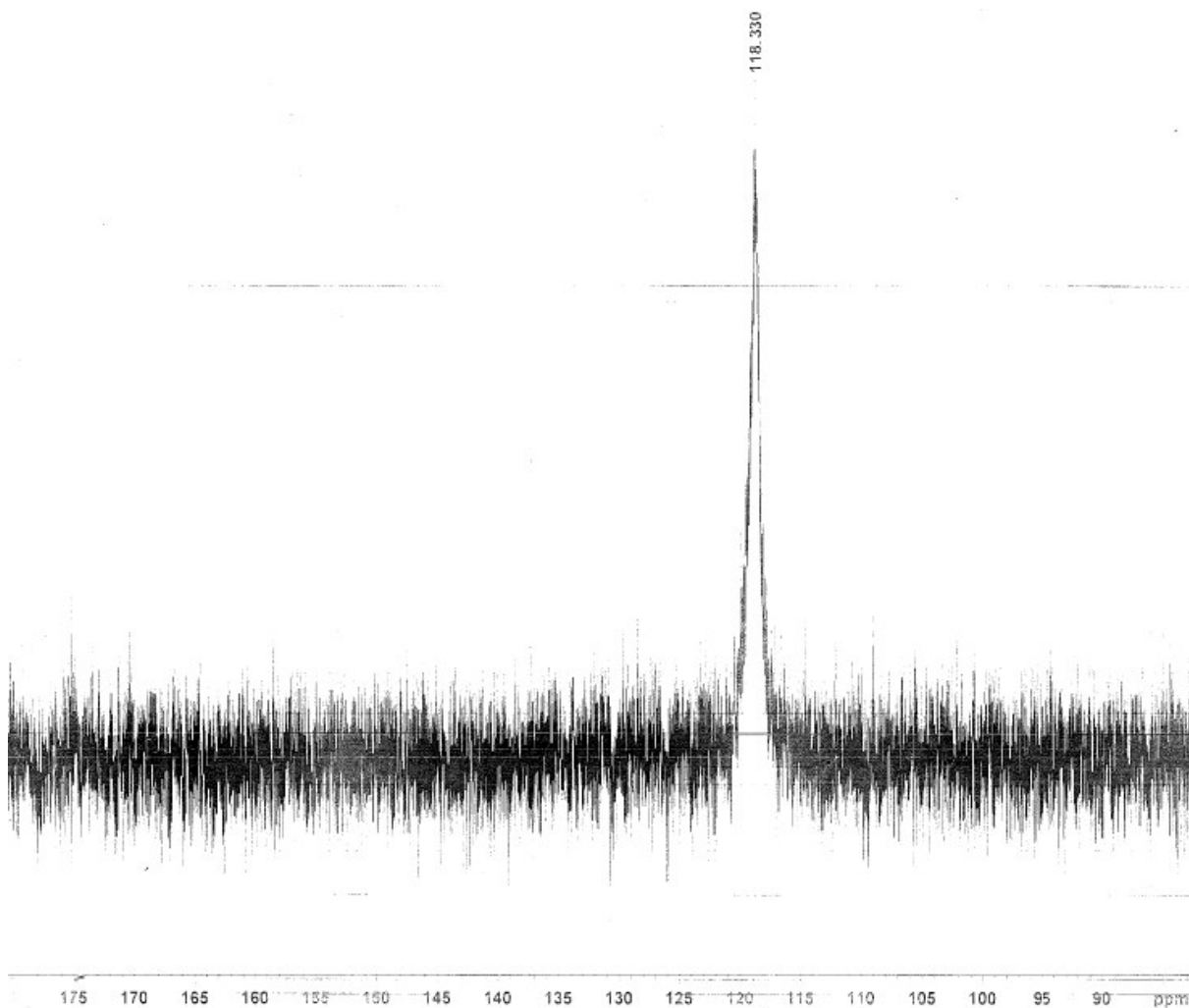


Figure S20. ^{31}P $\{\text{H}\}$ NMR spectrum (160 MHz, CD_3CN , 298 K) of **9**

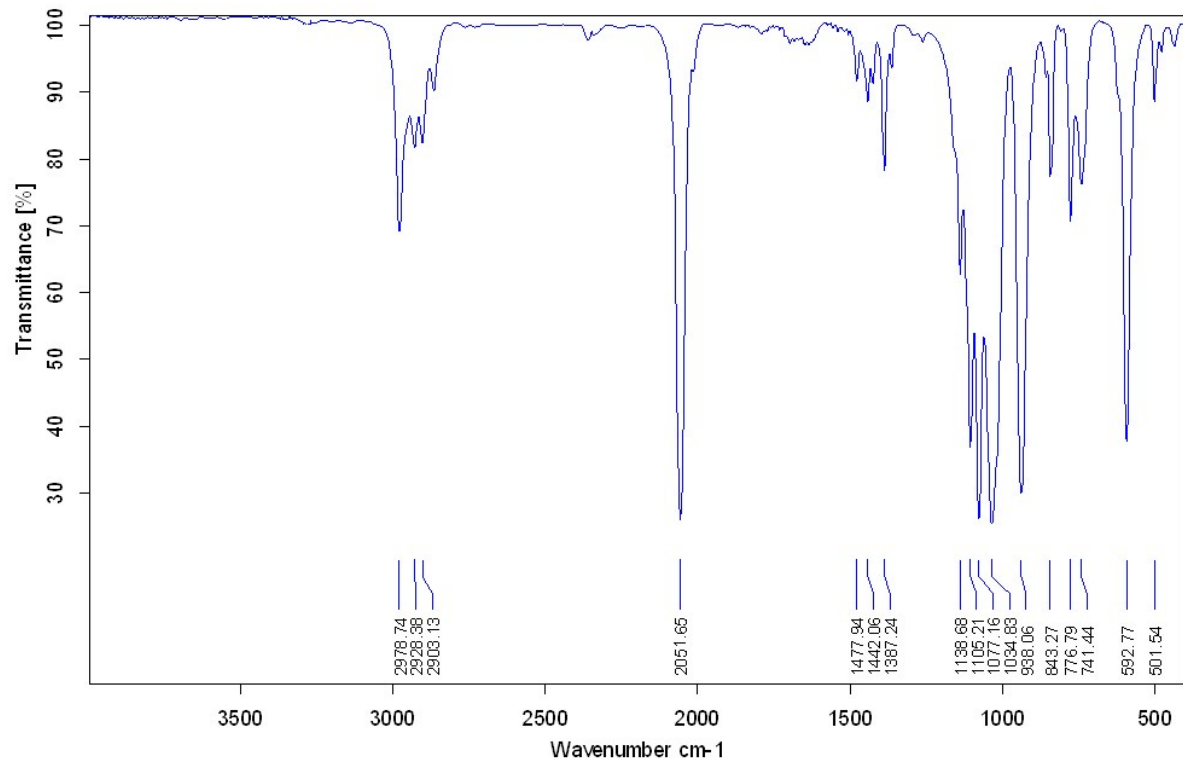


Figure S21. IR (KBr) spectrum of **2**.

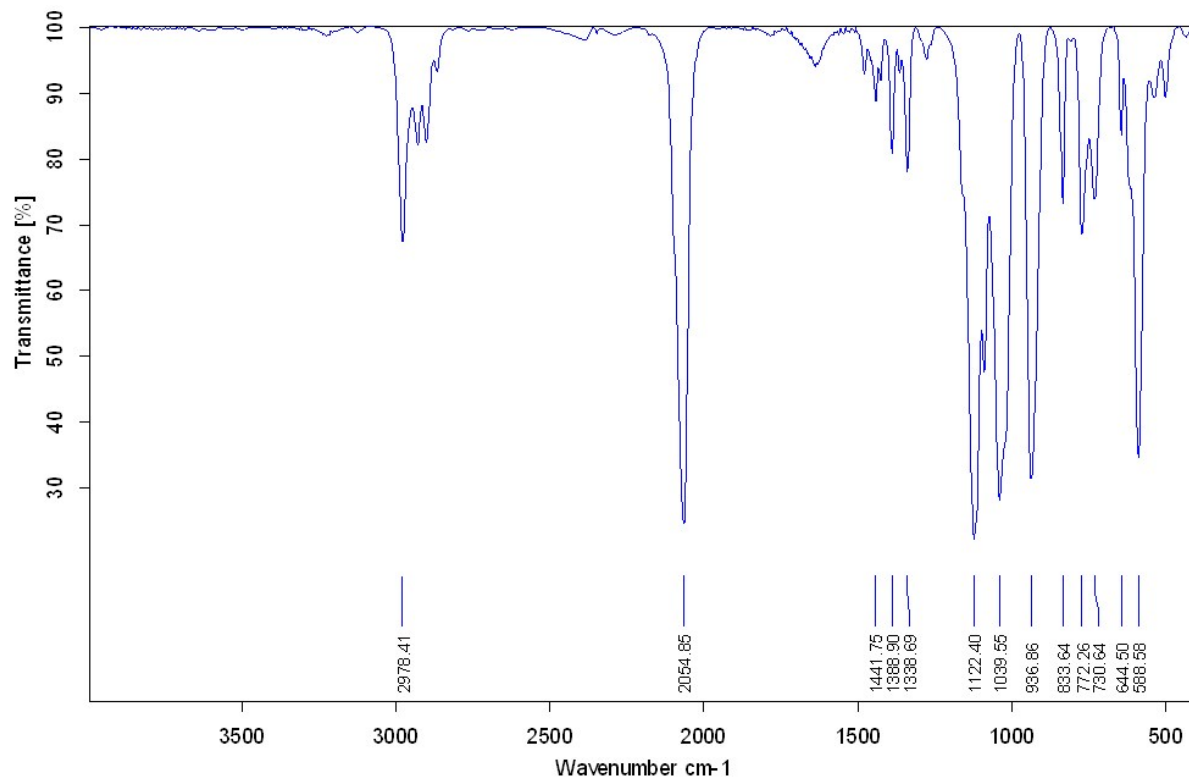


Figure S22. IR (KBr) spectrum of **3**.

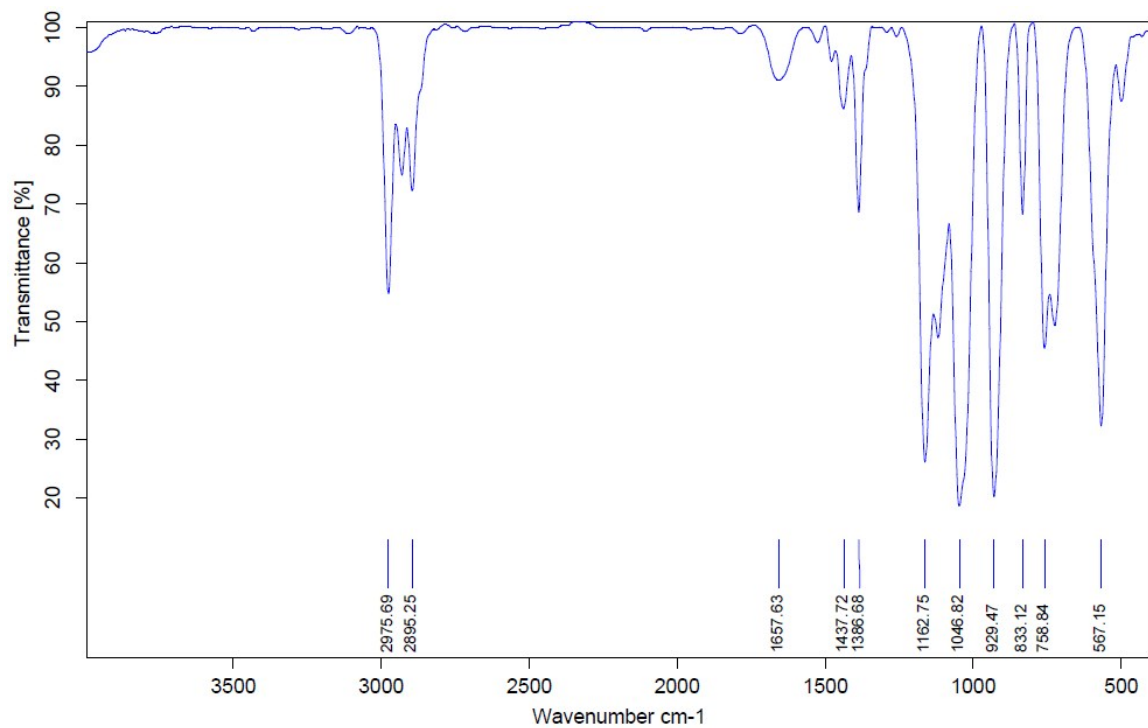


Figure S23. IR (KBr) spectrum of **4**.

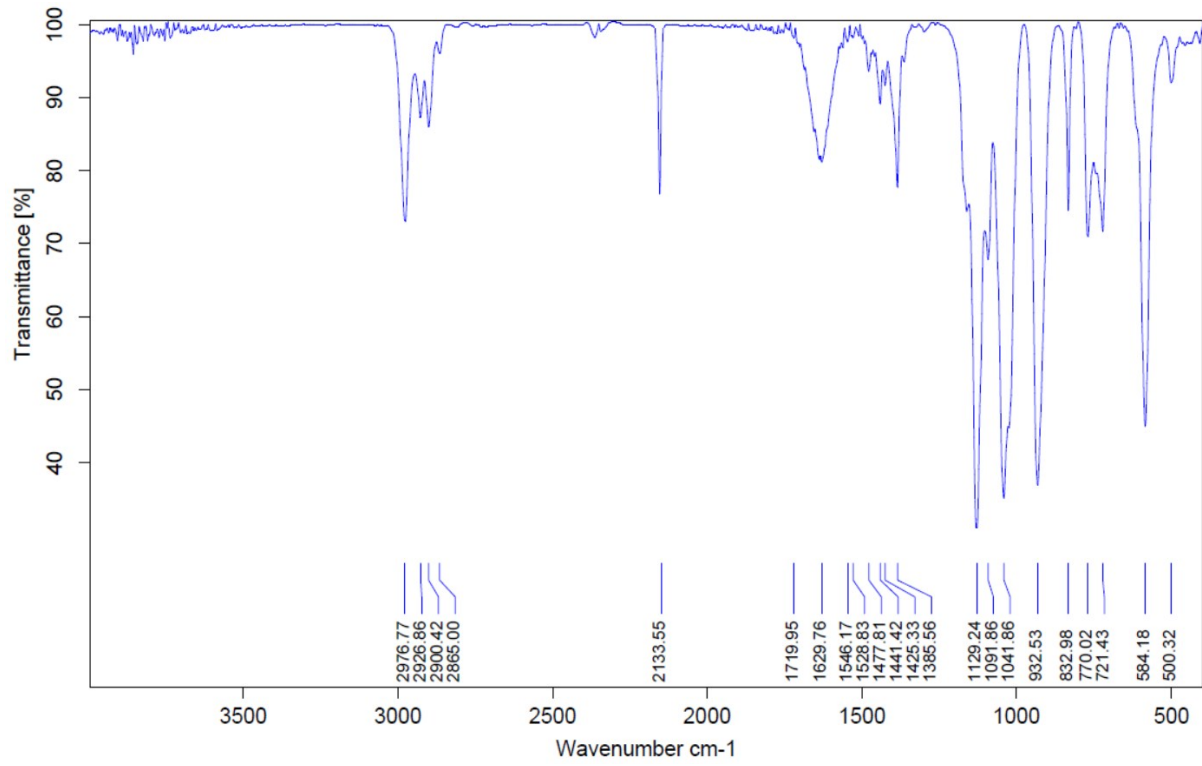


Figure S24. IR (KBr) spectrum of **5**.

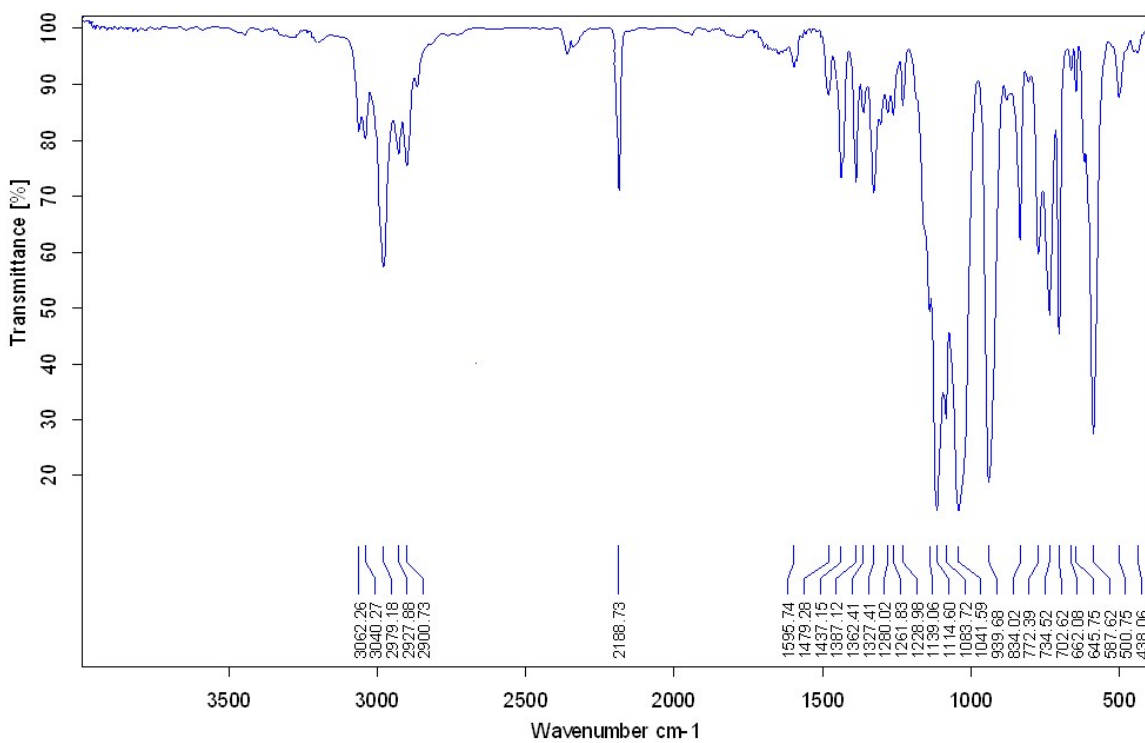


Figure S25. IR (KBr) spectrum of **6**.

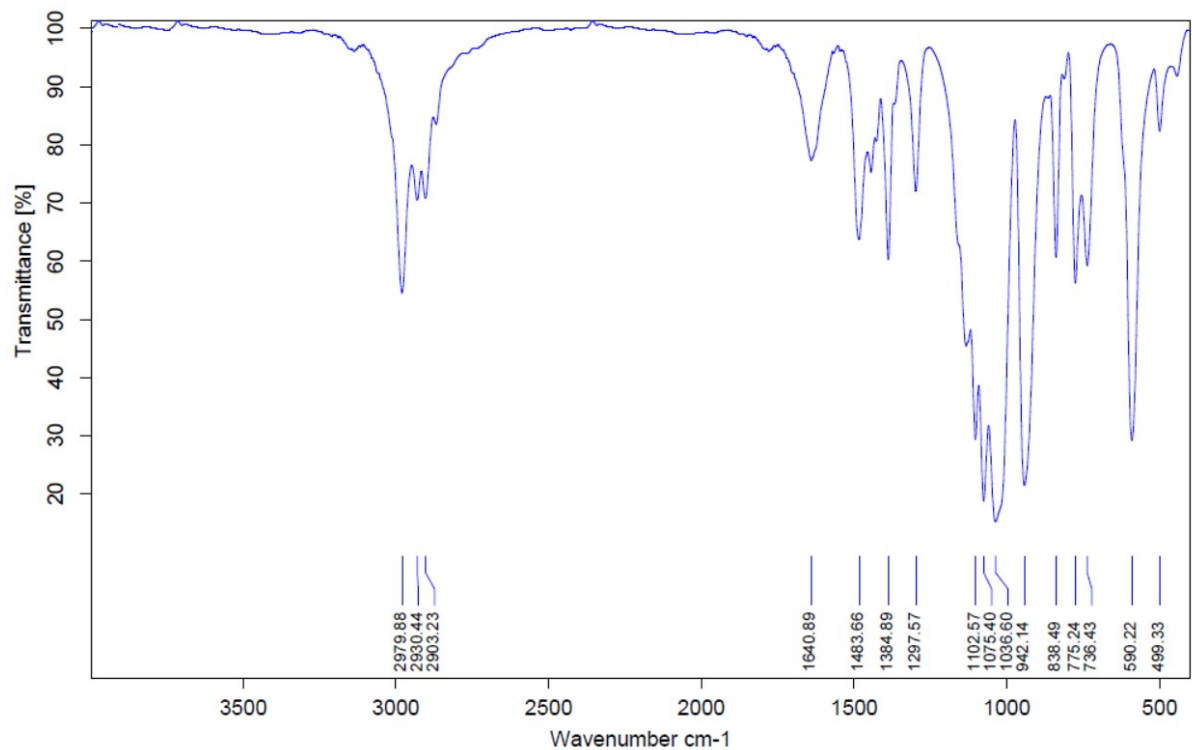


Figure S26. IR (KBr) spectrum of 7.

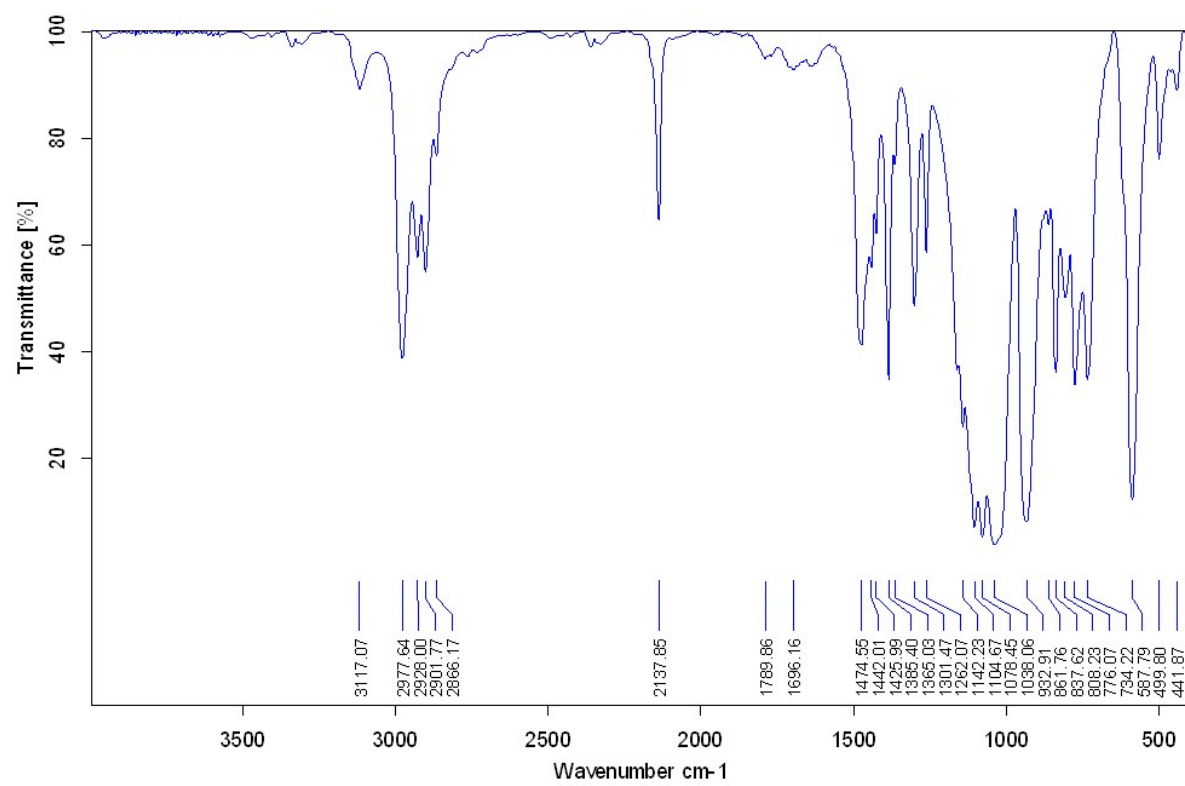


Figure S27. IR (KBr) spectrum of **8**.

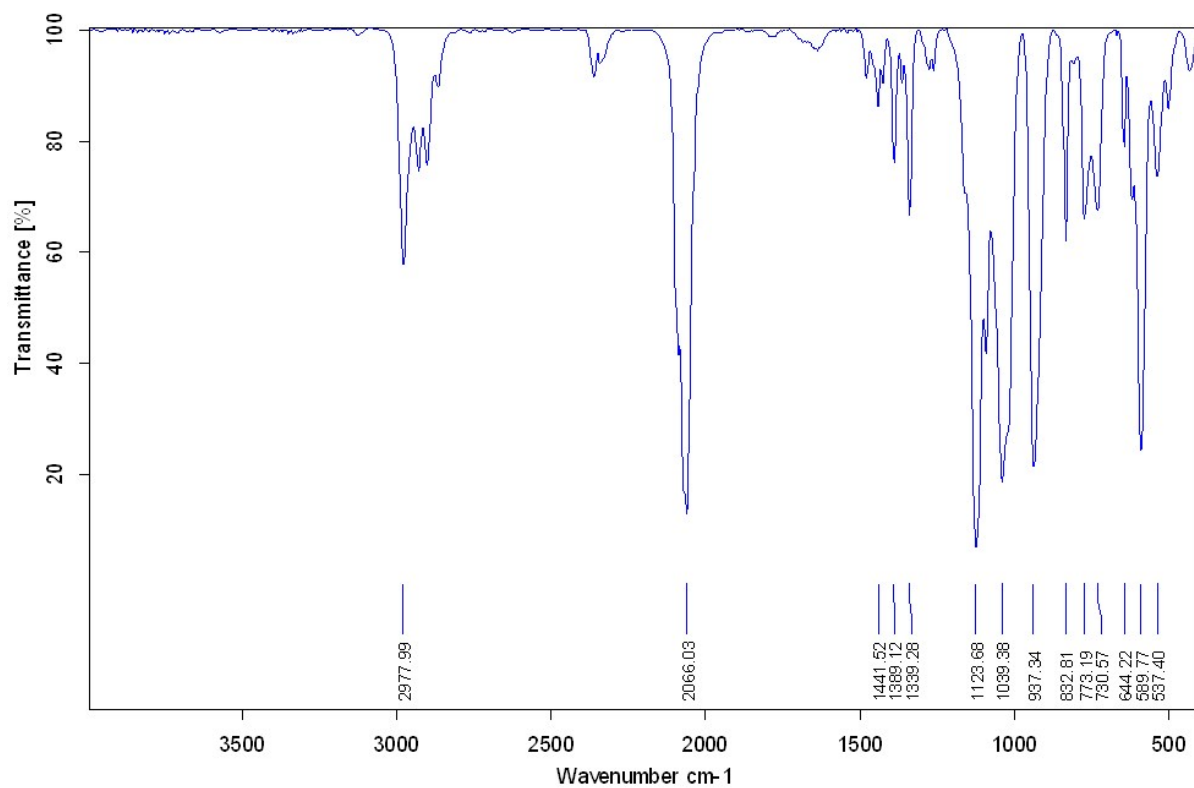


Figure S28. IR (KBr) spectrum of **9**.

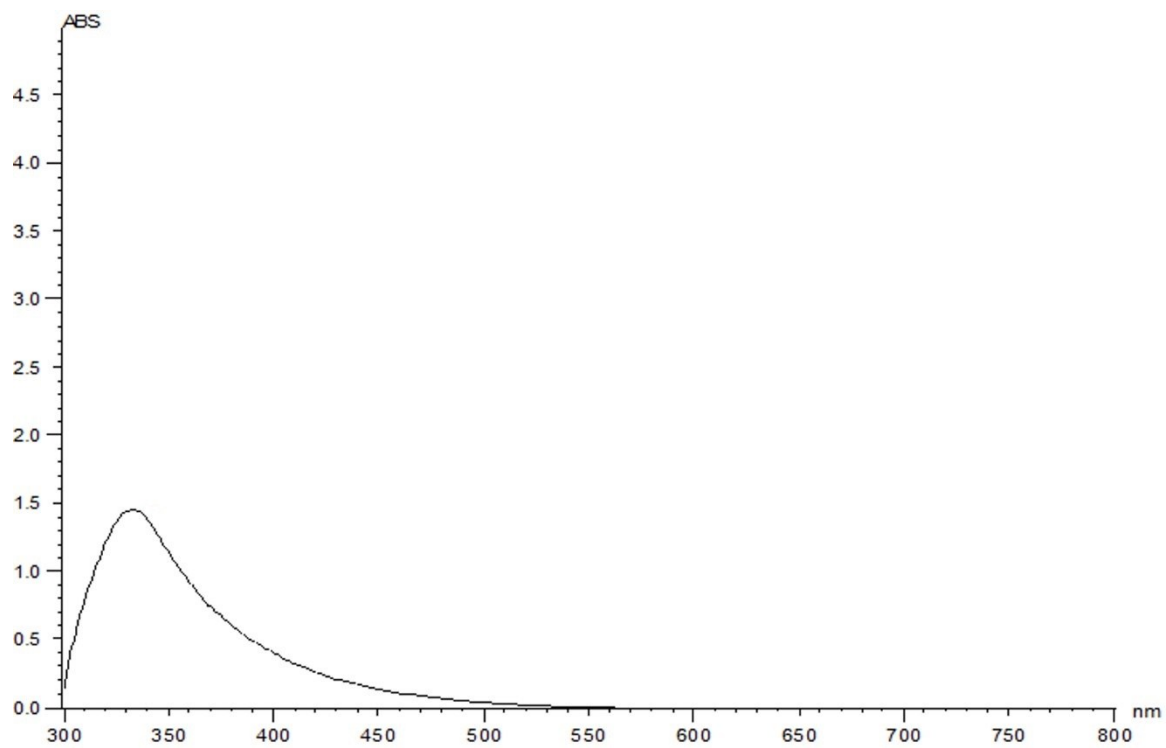


Figure S29. UV/Vis spectrum of **1** in MeCN.

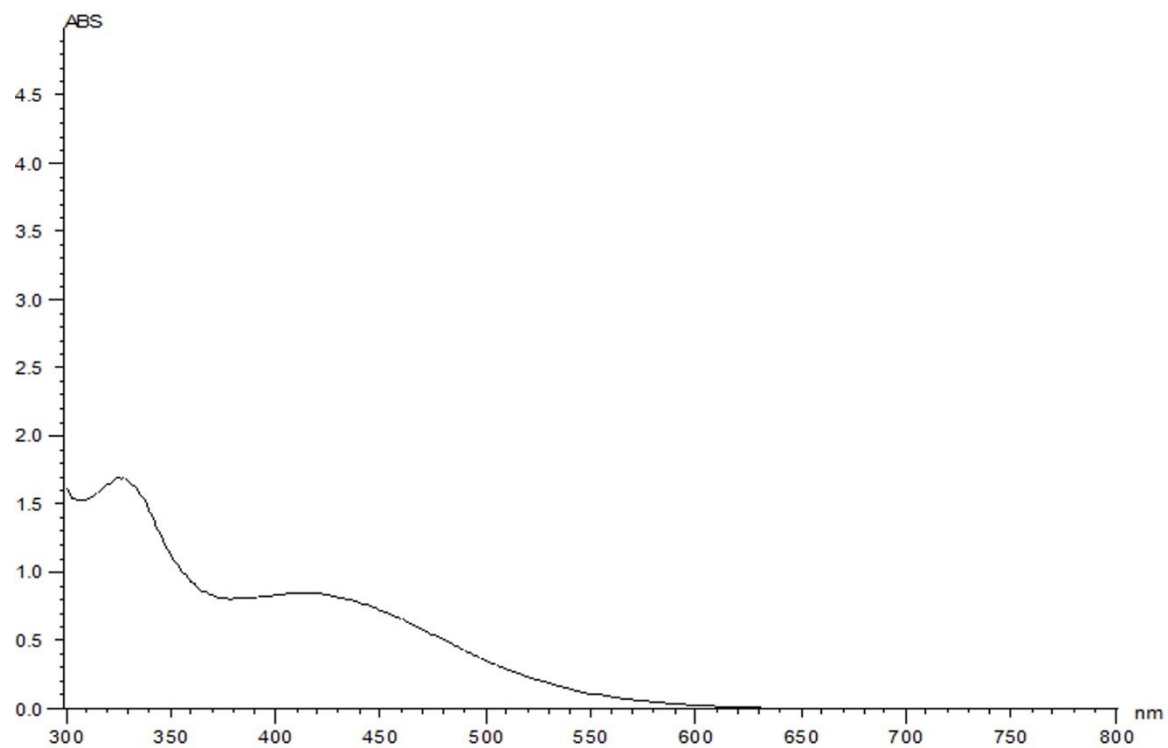


Figure S30. UV/Vis spectrum of **2** in MeCN.

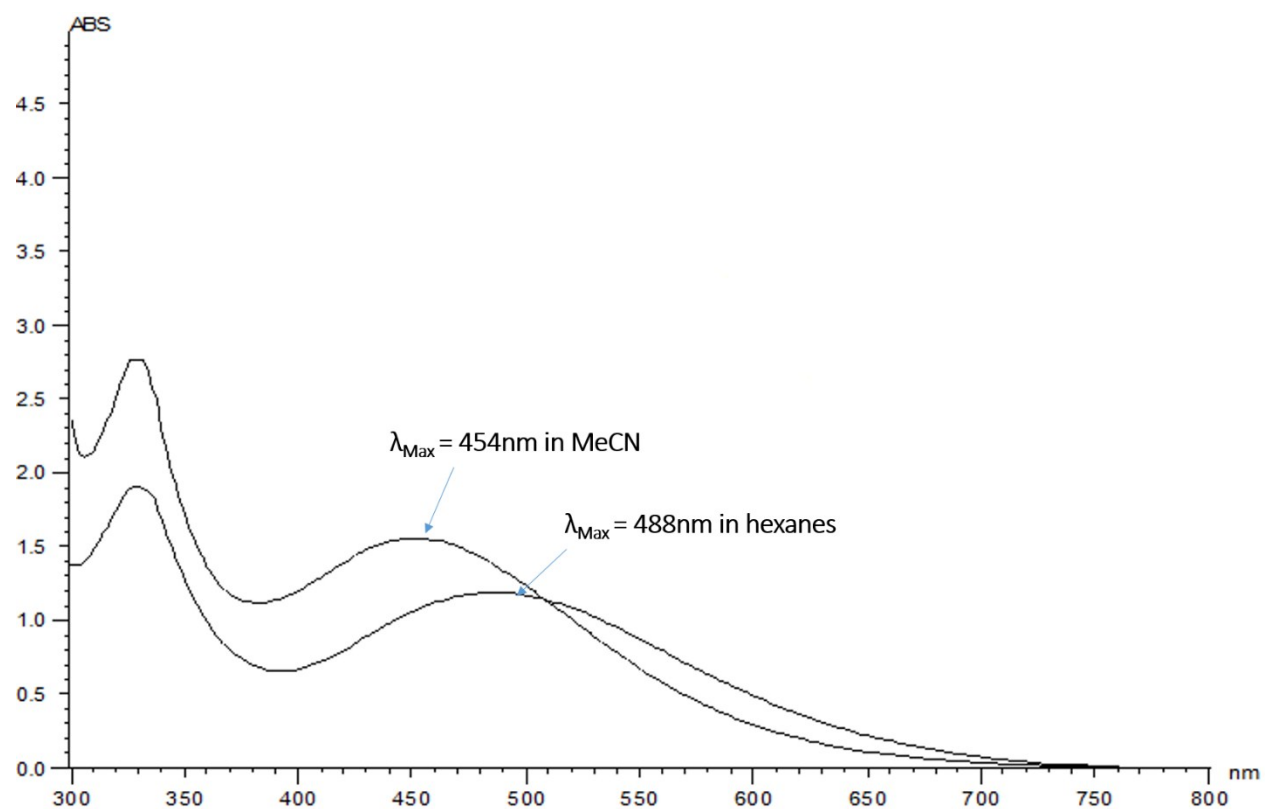


Figure S31. UV/Vis spectra of **3** in MeCN and hexanes

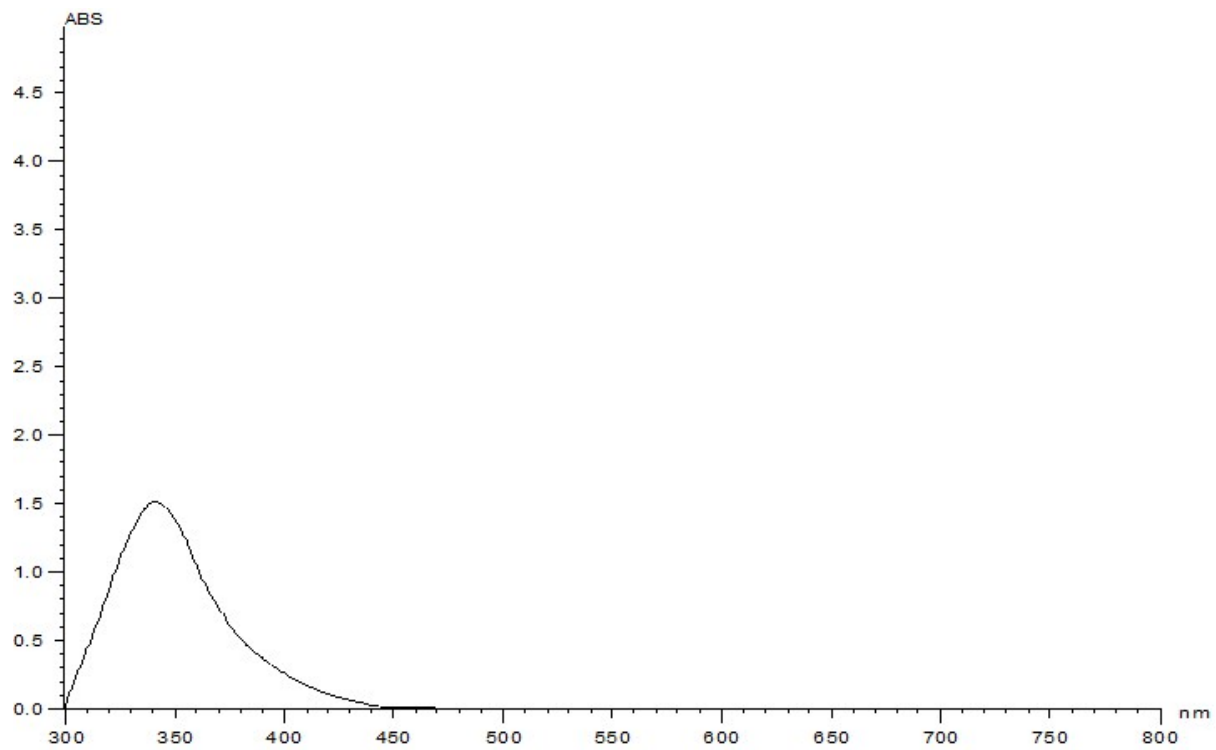


Figure S32. UV/Vis spectrum of **4** in MeCN.

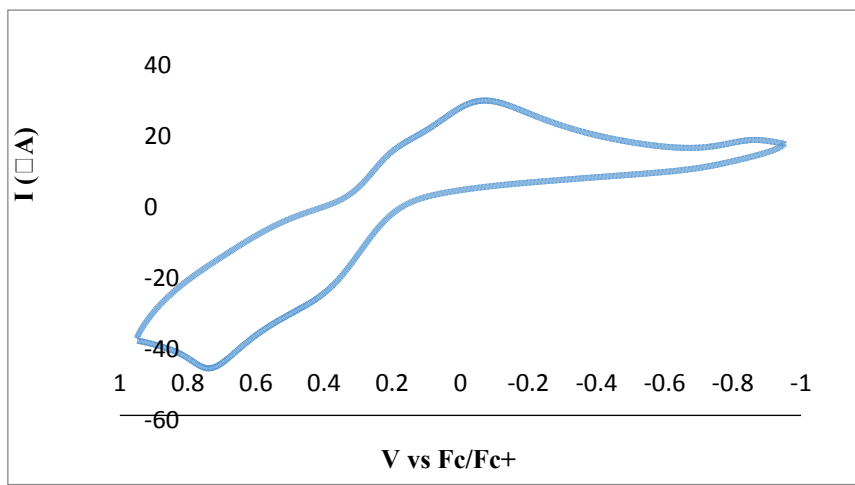


Figure S33. Cyclic voltammogram of $[\text{Ce}(\text{L}_{\text{OEt}})_2(\text{NCS})_2]$ (**2**) in MeCN with 0.1 M $[\text{Bu}_4\text{N}] \text{PF}_6$ (working electrode: glassy carbon electrode; scan rate = 100 mV s⁻¹).

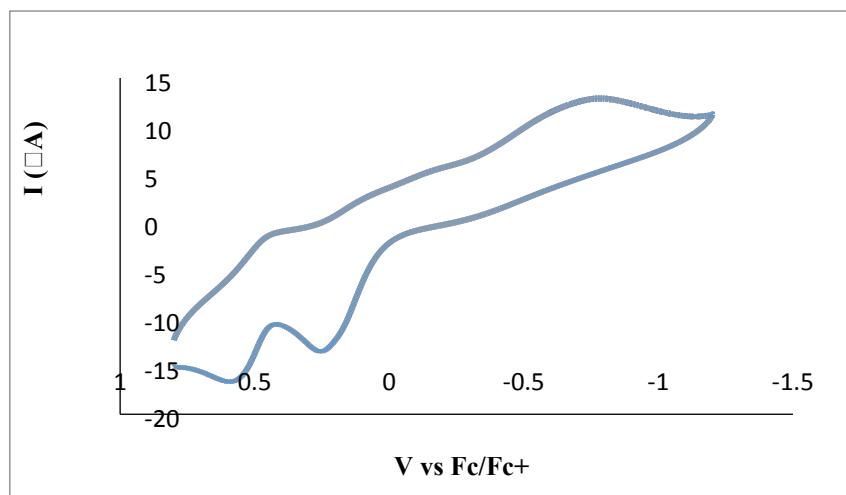


Figure S34. Cyclic voltammogram of $[\text{Ce}(\text{LOEt})_2(\text{N}_3)_2]$ (**3**) in MeCN with 0.1 M $[^n\text{Bu}_4\text{N}]^+\text{PF}_6^-$ (working electrode: glassy carbon electrode; scan rate = 100 mVs⁻¹).